IDENTIFICATION OF SATURN'S MAGNETOSPHERIC REGIONS AND ASSOCIATED PLASMA PROCESSES: SYNOPSIS OF CASSINI OBSERVATIONS DURING ORBIT INSERTION

N. André[1,2,3], M. Blanc[3], S. Maurice[3], P. Schippers[3], E. Pallier[3], T. I. Gombosi[4], K. C. Hansen[4], D. T. Young[5], F. J. Crary[5], S. Bolton[5], E. C. Sittler[6], H. T. Smith[7], R. E. Johnson[7], R. A. Baragiola[7], A. J. Coates[2], A. M. Rymer[8], M. K. Dougherty[9], N. Achilleos[9], C. S. Arridge[9], S. M. Krimigis[8], D. G. Mitchell[8], N. Krupp[10], D. C. Hamilton[11], I. Dandouras[3], D. A. Gurnett[12], W. S. Kurth[12], P. Louarn[3], R. Srama[13], S. Kempf[13], H. J. Waite[5], L. W. Esposito[14], and J. T. Clarke[15]

N. André, Research and Scientific Support Department, European Space Agency, Keplerlaan 1, PO Box 299, 2200 Noordwijk, The Netherlands (nandre@rssd.esa.int).

M. Blanc, I. Dandouras, P. Louarn, S. Maurice, P. Schippers, and E. Pallier, Centre d'Etude Spatiale des Rayonnements, 9 avenue du Colonel Roche, 31028 Toulouse, France.

T. I. Gombosi, K. C. Hansen, Center for Space Environment Modeling, Department of Atmospheric, Oceanic and Space Sciences, The University of Michigan, Ann Arbor, Michigan, 48109, USA.

S. Bolton, F. J. Crary, D. T. Young and H. J. Waite, Southwest Research Institute, San Antonio, TX 78238, USA.

R. A. Baragiola, R. E. Johnson, H. T. Smith, Enginnering Physics Program and Astronomy Department, University of Virginia, Charlottesville, VA 22904, USA.

E. C. Sittler, NASA/Goddard Space Flight Center, Greenbelt, MD 20771, USA.

A. J. Coates, University College London, Mullard Space Science Laboratory, Holmbury St. Mary, Dorking, Surrey RH5 6NT, UK.

N. Achilleos, C. S. Arridge, and M. K. Dougherty, The Blackett Laboratory, Imperial College, London SW7 2BZ, UK.

S. M. Krimigis, D. G. Mitchell, and A. M. Rymer, Johns Hopkins University Applied Physics Laboratory, 11100 Johns Hopkins Road, Laurel, MD 20723-6099, USA.

N. Krupp, Max-Planck Institut für Sonnensystemforschung, Max-Planck-Str. 2, D-37191 Katlenburg-Lindau, Germany.

Saturn's magnetosphere is currently studied from the microphysical to the global scale by the Cassini-Huygens mission. During the first half of 2004, in the approach phase, remote sensing observations of Saturn's magnetosphere gave access to its auroral, radio, UV, energetic neutral atom and dust emissions. Then, on July 1, 2004, Cassini Saturn Orbit Insertion provided us with the first in-situ exploration of Saturn's magnetosphere since Voyager. To date, Saturn Orbit Insertion is the only Cassini orbit to have been described in common by all field and particle instruments. We use the comprehensive suite of Magnetospheric and Plasma Science instruments to give a unified description of the large-scale structure of the magnetosphere during this particular orbit, identifying the different regions and their boundaries. These regions consist of the Saturnian ring system (Region 1, within 3 Saturn radii (R_s)) and the cold plasma torus (Region 2, within 5-6 R_s) in the inner magnetosphere, a dynamic and extended plasmasheet (Region 3), and an outer high-latitude magnetosphere (Region 4, beyond 12-14 R_s). We compare these observations to those made at the time of the Voyager encounters. Then, we identify some of the dominant chemical characteristics and dynamical phenomena in each of these regions. The inner magne-

D. C. Hamilton, University of Maryland, College Park, Maryland, USA.

D. A. Gurnett and W. S. Kurth, University of Iowa, Department of Physics and Astronomy, Iowa City, IA 52242, USA.

R. Srama and S. Kempf, Max Planck Institute Nuclear Physics, Saupfercheckweg 1, Heidelberg, 69117 Germany..

L. W. Esposito, LASP University of Colorado, 392 UCB, Boulder, C0 80309-0392, USA..

J. T. Clarke, Boston University, 725 Commonwealth Avenue, Boston, MA 02215 , USA

[1]Research and Scientific Support

tosphere is characterized by the presence of the dominant plasma and neutral sources of the Saturnian system, giving birth to a very special magnetosphere dominated by water products. The extended plasmasheet, where the ring current resides, is a variable region with stretched magnetic field lines and contains a mixture of cold and hot plasma populations resulting from plasma transport processes. The outer high-latitude magnetosphere is characterized by a quiet magnetic field and an absence of plasma. Saturn Orbit Inser-

Department, European Space Agency, Noordwijk, The Netherlands.

[2]University College London, Mullard Space Science Laboratory, Dorking, Surrey, UK.

[3]Centre d'Etude Spatiale des Rayonnements, Observatoire Midi-Pyrénées, Toulouse, France.

[4]Center for Space Environment Modeling, Department of Atmospheric, Oceanic and Space Sciences, The University of Michigan, Ann Arbor, Michigan, USA.

[5]Southwest Research Institute, San Antonio, Texas, USA.

[6]NASA Goddard Space Flight Center, Greenbelt, Maryland, USA.

[7]Engineering Physics Program and Astronomy Department, University of Virginia, Charlottesville, Virginia, USA.

[8]Johns Hopkins University Applied Physics Laboratory, Laurel, Maryland, USA.

[9]The Blackett Laboratory, Imperial College, London, UK.

[10]Max-Planck Institut für Sonnensystemforschung, Lindau, Katlenburg-Lindau, Germany.

[11]University of Maryland, College Park, Maryland, USA.

[12]University of Iowa, Department of Physics and Astronomy, Iowa City, Iowa, USA.

[13]Max Planck Institute Nuclear Physics, Heidelberg, Germany.

[14]LASP University of Colorado, Boulder, Colorado, USA.

[15]Boston University, Boston, Massachusetts , USA.

tion observations enabled us to capture a snapshot of the large-scale structure of the Saturnian magnetosphere and of some of the main plasma processes operating in this complex environment. The analysis of the broad diversity of these interaction processes will be one of the main themes of Magnetospheric and Plasma Science during the Cassini mission.

1. INTRODUCTION

The Saturnian space environment, a small planetary system in its own right, is one of the most complex environment in our solar system, because it connects dynamically and chemically all the components of the Saturn system: the planet, its ring system, numerous satellites (more particularly the icy satellites and Titan) and includes various dust, neutral and plasma populations. In this observational review, we shall focus our attention on the latter population with a particular emphasis on its interplay with the other phases of matter in the cavity created by Saturn's magnetic field in the solar wind, the Saturnian magnetosphere.

The sources of magnetospheric plasma in the Saturnian system can be divided between external sources (the solar wind) and internal sources (Saturn's ionosphere, the ring system, the inner icy satellites, and Titan). The contribution of the latter is, by far, dominant. The thermal plasma freshly created by the internal sources is trapped by the planetary magnetic field and entrained by the fast planetary rotation around the planet. The centrifugal force resulting from the rapid overall rotation (1 Saturnian day lasts for approximately 10 hours and 39 minutes) confines the plasma towards the equatorial plane, giving rise to a thin disc of corotating plasma in the inner magnetospheric regions and stretching the magnetic field lines outwards. In steady state, since the plasma added locally cannot build up indefinitely, a circulation system is set up such that the plasma is either transported outward to the remote magnetospheric regions where it escapes into the interplanetary medium, or lost down the planetary field lines into the ionosphere.

The interplay of plasmas of various origins and properties with the three sources of main momentum in the Saturnian magnetospheric system: the solar wind, planetary rotation, and orbital motions, results in several different chemical and dynamic plasma regions. This very rich magnetospheric environment contains uniquely diverse regions compared with those observed elsewhere in the solar system. Understanding these regions, their equilibrium and dynamics, and their coupling via the transfer of mass, momentum, and energy at their interfaces constitute both observational and theoretical challenges. A staggering array of phenomena and processes is indeed shaping this magnetosphere, which we are only beginning to comprehend, step by step.

Our first view and preliminary understanding of Saturn's magnetosphere in the 20th century was based solely on the fly-by data returned by Pioneer 11 in 1979 and by the Voyager 1 and 2 spacecraft in 1980 and 1981, as well as on remote observations from the ground or from Earth orbit. However, the resulting picture was limited by the local time and latitudinal coverage of the flybys, as well as by the lack of ion composition measurements and by the limited energy-angle coverage of the plasma instruments. These limitations forced us to develop models of the physics and chemistry occurring in Saturn's magnetosphere that reproduced our limited set of observations and enabled us to gain new insights on the physical processes operating in this system. The plasma and neutral observations and the models developed during the pre-Cassini era have been reviewed by *Richardson* [1998]. The interested reader may also find in this article more information to understand the source and loss processes of plasma and neutrals in a magnetosphere.

After these encounters, the overall picture that emerged was one of a magnetosphere that takes an intermediate place between Jupiter and the outer gas giants, Uranus and Neptune, with neutrals dominating the mass and density as at Uranus and Neptune, but with plasma playing an important role in the magnetospheric dynamics as at Jupiter.

Like Jupiter, Saturn is a rapidly rotating planet and there is no doubt that the planetary rotation drives the magnetospheric dynamics to some extent. In addition, as all objects in the solar system, Saturn interacts with the solar wind which drives a part of the magnetospheric dynamics and possibly triggers major storms when solar perturbations hit the magnetosphere. Establishing the relative importance of these two drivers is an important aspect of magnetospheric research activities.

Twenty-three years after Voyager, the Cassini-Huygens spacecraft completed its seven-year journey to the ringed world. The whole orbital tour of Cassini in the Saturn system has been designed, and will be necessary, to address among others the main magnetospheric and plasma science objectives of the mission [e.g., *Blanc et al.*, 2002]. Writing an up to date article can be an endless effort when considering the rate of new observations gathered by the spacecraft as its orbit moves in different regions of the magnetosphere. Instead, we shall focus our attention on Saturn Orbit Insertion observations and integrate all the observations obtained by the full suite of Cassini Magnetosphere and Plasma Science (MAPS) instruments in order to provide a multi-instrumental identification and characterisation of the magnetospheric regions crossed by the spacecraft along this particular orbit, as well as the dominant physical processes at work in each of these regions. This will be the strong unifying theme of our paper. Our objective is to detail the richness of the data sets previously analysed separately and to demonstrate how they can be combined to obtain a unified cartography of the Saturnian magnetosphere and a deeper understanding of interdisciplinary aspects of this fascinating environment. In addition, we will illustrate to the general planetary communities how scientific information can be extracted from observations obtained by the particle and field instruments, not only in term of magnetospheric science, but also in term of planetary science. Hopefully, this review will give them the ability to better understand how they can serve their own disciplines,

2. PRE-CASSINI PICTURE

Saturn's magnetospheric regions were first sampled by Pioneer and later analyzed in detail by the field and particle instruments carried by Voyager 1 and 2. A synthetic picture of Saturn's magnetosphere given by these observations has been described in *Sittler et al.* [1983] from a survey of the low-energy plasma (< 6 keV) environment. Although this picture was limited by the local time and latitudinal coverage of the Voyager fly-bys and by the energy coverage of the Voyager low-energy PLaSma instrument (PLS) and Low Energy Charged Particles (LECP) experiment, it provided us with the most comprehensive view for decades, until the arrival of Cassini, and presents a good context for the Cassini observations described in our next sections.

Three fundamentally different plasma regimes were identified at that time. We begin with the innermost regions and move outwards. All distances are expressed in Saturn radii (1 R_s=60,268 km):

- the inner plasma torus (inside 8 R_s) appeared as a region of low temperatures and high equatorial densities. This region is coupled to the ring system and icy satellites as the main sources of plasma, resulting from the dissociation of water molecules sputtered from the surfaces of icy satellites and rings, and protons from various origins (the solar wind, the atmospheres of Titan and Saturn as well as products of the water physical chemistry). Temperatures and flow speeds correspond closely to pick-up energies and corotation out to about 6 R_s, whereas the plasma moves more slowly than corotation outside 6 R_s as observed by Voyager 1 but not by Voyager 2. High-energy electrons were observed to be severely depleted. Interactions with dust, neutral gas or plasma ions and plasma waves may contribute to this depletion;

- the extended plasma sheet (between 8 and 15 R_s) was found to be composed of cold and hot plasma populations. In contrast with the local character of the plasma sources in the inner plasma torus, the cold plasma composition of this region appeared relatively homogeneous, suggesting that efficient mechanisms are operating in order to redistribute the plasma throughout the entire magnetosphere. The cold plasma population is found to dominate the density, whereas the hot plasma population dominates the pressure. Flow speeds were observed to progressively depart from corotation with increasing distance and to display a significant subcorotation. A ring current carried by charged particles of tens of keV trapped in Saturn's magnetic field was identified in this region. Cold plasma blobs centrifugally detached from the outer boundary of this ring current were believed to fill in the outer magnetosphere [*Goertz*, 1984];

- the hot outer magnetosphere (beyond 15 R_s) appeared as a highly time-variable region, dominated by hot plasma which is not centrifugally confined to the vicinity of the equatorial plane as is the cold plasma. Very irregular plasma structures were detected in this region by Voyager 1, at low latitudes. The structure of this region is probably highly variable with solar wind conditions. An other source of variability was also related to the presence of Titan, Saturn's largest moon, which orbits at about 20 R_s. The large atmosphere of Titan was indeed found to extend into a vast hydrogen torus atomic hydrogen, believed to be a relatively important plasma source [*Eviatar et al.*, 1983];

After the Voyager encounters, several puzzling issues remained open. Three of them, which will be discussed in our next sections, are briefly summarized below.

First, full consistency between available data and model estimates was not reached. Hubble Space Telescope (HST) observations revealed that large neutral OH densities are present in Saturn's magnetosphere [*Shemansky et al.*, 1993]. The sputtered neutral source required by plasma transport and chemistry models [10^{28} H_20/s, *Richardson and Jurac*, 2005] to explain these observations was found to be more important by one order of magnitude than estimated using Voyager LECP data. Satellite sputtering can only provide a fraction of the water needed [*Jurac et al.*, 2001a; *Paranicas et al.*, 2004]. To solve this inconsistency, *Jurac et al.* [2001b] suggested that very small ring grains in the E-ring (3-8 R_s) could provide a sufficient source of neutrals. In addition, *Jurac et al.* [2002] showed also that a vast majority of water molecules originates from Enceladus' orbit (3.95 R_s), possibly due to presence of an unknown population of colliding small bodies in the vicinity of the icy moon. This missing water source was poorly understood, waiting for new observations from Cassini.

Second, the mechanisms responsible for the outward transport in Saturn's magnetosphere are probably diverse and operate through different modes and on different scales as a function of radial distance. In a magnetosphere dominated by neutrals like that of Saturn, fast neutral transport through charge-exchange may be undoubtedly at play and subsequent re-ionization in the outer magnetosphere of the water-group neutrals initially originating from the inner magnetosphere may be important. The other key process long believed to be an important aspect of outward plasma transport in a rapidly rotating magnetosphere like that of Saturn is the development of the centrifugal interchange instability (a Rayleigh-Taylor type instability with the centrifugal force playing the role of gravity) [*Melrose*, 1967]. Evidence for this process at Saturn was lacking before the arrival of Cassini, but its signatures were identified at Jupiter [*Bolton et al.*, 1997; *Kivelson et al.*, 1997; *Thorne et al.*, 1997; *Russell*, 2004] using observations from the Galileo spacecraft, lending confidence to the hypothesis that it is a common process in giant planet magnetospheres.

Third, a remarkable feature of Saturn's intrinsic magnetic field identified from these past observations was the very close alignment of its magnetic dipole axis with the planetary spin axis [*Smith et al.*, 1980]. Therefore, unlike Jupiter, the rotational modulation of Saturn's magnetic field should be very small, essentially reflecting the effects of non-axisymmetric terms of the Saturnian magnetic field. However, rotational modulation effects are probably significant since a planetary spin modulation was observed on radio emissions [Saturn Kilometric Radiation (SKR), *Warwick et al.*, 1981] and energetic particle fluxes [*Carbary and Krimigis*, 1982]. The spin period of Saturn was determined by Voyager and was commonly accepted to be 10 hours, 39 minutes, 24 ± 7 seconds. This value was inferred from the radio emissions, since the internal rotation period of giant gaseous planets can not be accurately determined from visual observations. However, *Galopeau and Lecacheux* [2000] analyzed Ulysses' observations of SKR and found a striking difference between the results obtained from Voyager and those obtained from Ulysses, with a period deduced from Ulysses' observations that is fluctuating with time and may differ by 1% from that deduced from Voyager observations 18 years earlier. Since *Galopeau et al.* [1995] interpreted the source locations of SKR in terms of electron precipitations possibly caused by the Kelvin-Helmholtz instability arising on the morningside flanks of the Saturnian magnetopause (this instability resulting from the velocity shear between the solar wind and the corotating magnetospheric plasma), *Galopeau and Lecacheux* [2000] proposed that a motion of the SKR radio sources originating from the modulation of the solar wind may explain the fluctuations of the radio period. Re-analyzing Pioneer and Voyager magnetometer data, *Espinosa et al.* [2003a] found later evidence for planetary-period magnetic field oscillations in Saturn's magnetosphere. *Espinosa et al.* [2003b] tentatively suggested that Saturn presents an equatorial anomaly restricted in longitude, which generates a compressional outward propagating wave as the planet rotates. Also, the existence of a high latitude magnetic anomaly in the near-surface Saturnian field was postulated years before by *Galopeau et al.* [1991] based on their analysis of the SKR high-frequency limit. All these observations suggested that a basic rotational asymmetry must exist in the Saturnian magnetosphere, which should be identified with the help of Cassini data, in addition to the basic dayside/nightside asymmetry (local time effects) that results from the interaction of the solar wind with Saturn's magnetic field.

3. THE CASSINI MAPS INSTRUMENT SUITE

The Cassini-Huygens complement of plasma and field instruments allows measurements of the magnetic field by the Magnetometer (MAG) instrument [*Dougherty et al.*, 2004], of a very broad range of charged and neutral particle populations by the Magnetospheric Imaging Instrument (MIMI) and Cassini Plasma Spectrometer (CAPS) instruments [*Krimigis et al.*, 2004; Young et al., 2004] and of the dynamic spectra of plasma waves and radio emissions by the Radio and Plasma Wave Science (RPWS) instrument [*Gurnett et al.*, 2004]. Several other particle populations which are of central interest for Saturn's magnetosphere are also measured by Cassini [cf. Table X in *Blanc et al.*, 2002]. The Cosmic Dust Analyser (CDA) instrument measures cosmic dust particles of Saturnian or interplanetary origin [*Srama et al.*, 2004]. The Ion Neutral Mass Spectrometer (INMS) instrument measures particles from the ionospheres and neutral atmospheres of Titan, the rings and the other satellites [*Waite et al.*, 2004]. Finally, the Ultraviolet Imaging Spectrograph (UVIS) instrument can remotely detect ultraviolet emissions from the orbital neutral clouds of Saturn [*Esposito et al.*, 2004]. Other optical remote sensing instruments can contribute indirectly to Magnetosphere and Plasma Science, and the interested reader is referred to the Cassini-Huygens mission Space Science Reviews volume(s) [*C. T. Russell*, 2004] for more details.

The dual-technique Magnetometer (MAG) instrument on-board Cassini consists of two separate magnetometers: 1) a helium magnetometer operating in either a vector (VHM) or scalar (SHM) mode, 2) and a fluxgate magnetometer (FGM), mounted at the end and halfway down a 11-meter boom, respectively. The MAG instrument has the ability to measure magnetic fields up to 256 nanoTeslas (nT) when using the VHM, from 256 to 16,384 nT with the SHM, and up to 44,000 nT when using the FGM.

The CAPS instrument comprises three sensors: 1) an Ion Mass Spectrometer (IMS) that measures ion energy per charge between 1 electronVolt (eV) and 50 keV, 2) an Electron Spectrometer (ELS) that measures electron energy from 1 eV to 28 keV, and 3) an Ion Beam Spectrometer (IBS) that measures ion energy per charge with an higher resolution and is appropriate for narrowly beamed distributions. The instrument is mounted onto a turntable that rotates around the spacecraft Z-axis in order to enlarge the coverage in the azimuthal direction.

The MIMI instrument comprises three sensors: 1) the Low Energy Magnetospheric Measurement System (LEMMS) that detects energetic ions from 20 keV to 18 MeV and energetic electrons from 15 keV to 1 MeV, 2) the Charge Energy Mass Spectrometer

(CHEMS) that detects ions from 3 to 230 keV per charge and allows for the identification of their charge state, and 3) the Ion and Neutral Camera (INCA) that detects ion and neutral species from 7 to 200 keV per nucleon. The LEMMS instrument is also mounted on a turntable that rotates around the Y-axis of the spacecraft every 86 s in order to provide good pitch angle coverage.

The RPWS instrument comprises several antennas that measure the electric and magnetic fields of radio emissions and plasma waves, from 1 Hertz (Hz) to 16 MHz for electric fields, and from 1 Hz to 12 kHz for magnetic fields. It also includes a Langmuir probe to measure the density and temperature of the local plasma.

The CDA instrument consists of two independent dust detection systems: 1) the Dust Analyser measures particles with large mass (from 10^{-18} to 10^{-12} kilograms) and velocity range (from 1 to 100 kilometers per second), and 2) a High Rate Detector is designed for dust-rich environments (up to 10^4 impacts per second) and determines particle mass for particles with a known speed.

The INMS instrument consists of a closed ion source for the measurement of neutrals that do not react with the antechamber surfaces of the instrument and an open ion source for the measurement of reactive neutrals and ions. The instrument samples ambient dense neutral and low-energy (below 100 eV) ion populations, with a mass range from 1 to 99 atomic mass units.

The UVIS instrument comprises several telescope-spectrographs operating in the extreme and far ultraviolet domains (with spectral bands covering a wavelength range from 55.8 to 190 nanometers) and is designed to remotely detect emissions from atomic oxygen, and molecular and atomic hydrogen.

4. APPROACH PHASE

During the last months before SOI, Cassini-Huygens was first able to combine remote sensing observations of the Saturn system with in-situ measurements of the solar wind. We shall briefly review these data, complemented by HST observations of Saturn's aurora, which provide a unique opportunity to study the Saturnian magnetosphere as an astrophysical object, observed from a distance through its various emissions. From January 2004, Cassini's approach was from the morning side of the planet, near a local time of $\sim$7 hours at distances of up to 1450 Saturn radii or 87 million km.

The most spectacular of these observations are probably the HST observations of Saturn's UV aurora, which provided a unique set of data during the dedicated January 2004 observation campaigns [*Clarke et al.*, 2005]. This data set revealed highly variable auroral emissions, likely to be at least partly controlled by the solar wind as the comparison with in-situ measurements of the solar wind and interplanetary magnetic field by Cassini suggested [*Crary et al.*, 2005; *Belenkaya et al.*, 2006]. In contrast to Earth, the main controlling factor appears to be the solar wind dynamic pressure, with the orientation of the interplanetary magnetic field playing a much more limited role. At Saturn, the interplanetary magnetic field is weaker and the magnetosheath hotter, therefore reconnection should be less efficient than at Earth [*Leisner et al.*, 2007].

The RPWS data complemented the auroral observations by providing remote sensing data of the radio component of Saturn's auroral emissions, the Saturn kilometric radiation (SKR). This emission, which is seen up to 1.2-1.3 Mhz in the RPWS dynamic spectra, contains a wealth of information because it displays a double modulation. First the emission is modulated with the planetary rotation period, showing that the emitting system itself (e.g., the interplay of the magnetic field geometry, plasma characteristics and energetic electron fluxes which produces the emission via the so-called cyclotron maser instability) is longitudinally asymmetric or is modulated by the planetary rotation (Saturn, as a radio source, has been compared to a strobe light). Then, superimposed on this planetary rotation modulation, the SKR also varies in intensity over a longer time scale, in a way that large SKR variations correlate with UV ones [cf. Figure 1c of *Kurth et al.*, 2005a], while the solar wind dynamic pressure correlates much better and more extensively with SKR power [*Desch*, 1983 and many further studies - see review in *Zarka*, 1998].

From the UV and radio emission, one can infer a rather classic magnetosphere, in which solar wind/magnetosphere coupling plays an important role, but a longitudinal asymmetry of still yet unknown nature in the magnetic field and charged particle distribution is also important since the apparently axisymmetric magnetic field of Saturn, as deduced from Pioneer and Voyager observations, makes it difficult to understand the strong SKR modulation without appealing to the existence of a such an asymmetry.

A second, very different and rather unique, feature of Saturn's magnetosphere is revealed by two other types of emissions, the UV emission of its atomic oxygen cloud and its energetic neutral atom (ENA) emission. The observations of the neutral atomic oxygen emission by UVIS [*Esposito et al.*, 2005] revealed the presence of an extended atomic oxygen torus, peaking near the orbit of Enceladus up to ∼16 R_s in the orbital plane. UVIS also observed a very broad torus of neutral hydrogen that fills the entire magnetosphere, extending through the magnetopause (∼20 R_s at 12:00 local time). This torus observation complemented the pre-Cassini observations of the OH cloud, showing that Saturn's magnetosphere is immersed in a very extended cloud of neutral gas, apparently dominated by hydrogen and water products, and whose density even exceeds the local plasma density almost everywhere by at least one order of magnitude. Saturn's neutral/ion mixing ration (~ 10) is 3 to 4 orders of magnitude greater than at Jupiter [*Esposito et al.* 2005; *Delamere et al.*, 2007]. Neutral oxygen in the Saturnian system showed also variability. UVIS observed a transient event that produced O in the system, which could result from a single injection of neutral gas, which then dissipated within about 2 months. The ENA images, which show a very broad emission extending beyond the orbit of Titan, reveals in a different way the importance of the neutral gas population and its interaction with charged particles throughout the magnetospheric cavity [*Krimigis et al.*, 2005]. In these charge-exchange processes, neutral gas is removed from the system into the interplanetary medium while replacing old ions with new ions.

Finally, the CDA observations of high-velocity dust streams ($\leq$100 km$\cdot$s^{-1}) before and after the first crossing of Saturn's magnetosphere by Cassini showed that, just as Jupiter, Saturn's magnetosphere behaves as a giant dust particle accelerator [e.g., *Kempf et al.*, 2005]. Outside of these magnetospheres, the dynamics of charged dust particles are governed by their interaction with the interplanetary magnetic field. The main source of Jovian dust streams is Jupiter's moon Io and its volcanic activity. The characteristics and amplitude of the impact signals produced by Saturnian and Jovian dust streams in the CDA instrument are very similar, suggesting that the mass and impact speeds are at least comparable, with grain sizes below 10 nm. The observed composition of dust stream particles observed outside the magnetosphere, their energy, and specific trajectory calculations suggest that these particles originated near the outer edge of the main rings before being accelerated outward by the internal magnetospheric electric field associated with the diurnal rotation of the planetary magnetic field and background plasma (the so-called (radially oriented) corotation electric field). Remarkably, CDA enabled us to obtain information on the properties of Saturn's main ring particles, even at large distances from the ring system.

In summary, even before the SOI observations, several of the key features of Saturn's magnetosphere could be deduced from its broad variety of emissions: a magnetosphere with a significant modulation by planetary rotation, partly controlled by its interaction with the solar wind, with a strong natural corotation electric field accelerating dust particles outwards, and embedded in a broad neutral cloud of hydrogen and water products with local densities comparable to or significantly larger than the ionized population.

5. SATURN ORBIT INSERTION

Then, on July 1, 2004, Cassini-Huygens was successfully inserted into Saturn orbit. Figure 1 shows the trajectory of the Cassini spacecraft during SOI, together with the trajectories of Pioneer 11, Voyager 1 and 2, in terms of local time (LT) coverage (Figure 1, left panel) and distance to the Saturnian equatorial plane (Figure 1, right panel). The Cassini spacecraft encountered the Saturnian magnetosphere through its early morning sector, near 08:00 LT inbound and 04:00 LT outbound. The spacecraft stayed below the Saturnian equatorial plane during the majority of the flyby, except near closest approach (which occurred at 1.3 R_s) when it crossed this plane twice (around 2.6 R_s). There were no special close encounters with any of the Saturnian satellites during this orbit, apart from the unique pass through the ring system of the planet. As this figure shows, the three previous flybys provided a very limited local time coverage of the Saturnian magnetosphere, basically limited to the noon and early morning sectors, but some coverage in latitude.

Figure 1 enables us to compare the locations of the outer boundaries of the Saturnian magnetosphere, the magnetopause, which controls the coupling of the incident solar wind flow to the magnetosphere. The location of this boundary is determined by the dynamic pressure of the solar wind and the combined plasma and magnetic pressure of the magnetosphere. Since these pressures are strongly time variable, several magnetopause crossings were observed by the spacecraft (7 in total on the inbound and outbound passes, *Dougherty et al.* [2005]). The last inbound magnetopause crossing occurred at a radial distance of 30.7 R_s, 8 R_s below the equatorial plane, around 02:44 UT on June 29, whereas the first outbound one occurred at 34.5 R_s from the planet, 9.6 R_s below the equatorial plane, around 03:56 UT on July 4. When compared with the average *Arridge et al.*' [2006] empirical magnetopause model, based on magnetometer observations obtained during the first six orbits of Cassini, the last observed inbound crossing is located further from the planet than the model, the magnetosphere being more inflated at that time. On the contrary, the first observed outbound magnetopause crossing is located closer, the magnetosphere being more compressed at that time relative to the model. A survey of all the bow shock and magnetopause crossings observed during SOI indicated that the Saturnian magnetospheric boundaries appeared very dynamic [*Hendricks et al.*, 2005; *Hansen et al.*, 2005].

The overall context of solar wind and interplanetary conditions at the time of the arrival of Cassini in the Saturnian magnetosphere is discussed in detail by *Jackman et al.* [2005] and is shown to support this interpretation of two rather different states of the Saturnian magnetosphere during inbound and outbound Cassini observations due to the effect of the arrival at Saturn of a corotating interaction region (CIR) compression region. The structure of the interplanetary medium observed by Cassini en route to Saturn was found to be consistent with that expected to be produced by corotating interacting regions during the declining phase of the solar cycle. The observed highly structured nature of the interplanetary magnetic field generally consisted of two magnetic sectors per solar rotation, with crossings of the heliospheric current sheet usually embedded within high field compression regions lasting for a few days, surrounded by rarefaction regions lasting for several days and in which the field strength (and probably the density) is very low. As the compression regions reached the Saturnian magnetosphere, the solar wind pressure compressed the system. During SOI, *Jackman et al.* [2005] suggested that such a magnetospheric compression is likely to have occurred early on July 2.

We discuss in the next sections observations obtained 24 hours on either side of Cassini closest approach (CA, which occurred at a distance of 1.33 R_s, 02:40 UT on July 1). During the insertion burn manoeuver (at a distance of $\sim$2 R_s, 90 minutes prior to closest approach) and during some of the spacecraft rolls intended to satisfy safety and science operations (around closest approach +/- 2 h), some of the instruments were turned off as a precaution. Other obtained data are contaminated either by the noise from the rocket engine firing or by insufficient sensor orientation knowledge. Interestingly, five hours after the orbit insertion manoeuver, Cassini observed in-situ ion cyclotron waves (observation 7 in panel 3 of Figure 4) induced by its own engine exhaust gases (including CO_2, N_2, CO), ionized and accelerated by the magnetospheric rotation [*Russell et al.*, 2005]. The authors estimated that, when the engines fired, they produced a plume of over 850 kg of neutral gas that reached distances close to 5 R_s before the energy of the picked up ions reached a value sufficient to generate the strong waves observed.

6. A SINGLE INSTRUMENT APPROACH

The identification of the various Saturnian magnetospheric regions following SOI has been discussed from the point of view of each single instrument in various papers [*Dougherty et al.*, 2005; *Gurnett et al.*, 2005; *Krimigis et al.*, 2005; *Young et al.*, 2005; *Krupp et al.*, 2005]. Their characterization and the nomenclature used were based on the particular individual scientific objectives of each instrument and, hence, different regions and boundaries were identified. We shall summarize in this section what has been reported by each instrument separately.

Figure 2 represents observations from the MIMI LEMMS, MAG VHM, CAPS ELS, CAPS IMS, and RPWS sensors obtained on June 30 and July 1. Colour-coded energy-time and frequency-time spectrograms are used to represent particle and wave instrument observations, respectively. Low- and high-energy electron and ion observations are represented on two separate panels for the sake of clarity. Magnetospheric magnetic field components are described in a Saturn-centered polar spherical coordinate system. Before discussing this first unified picture, we start with a summary of the morphology of the magnetospheric plasma and fields described by each of the different instruments separately. Again, we begin with the outermost regions and move inwards. Observations are organized in the approximate chronological order.

1) The morphology of the magnetosphere has been identified with the help of the energetic particle observations (panels 1 and 2 of Figure 2) by looking at large-scale changes in energetic electron and ion intensities and their variations [*Krimigis et al.*, 2005]. These

features enabled *Krimigis et al.* to distinguish three distinct regions both on the inbound and outbound passes:

- the lobes, where the energetic particle intensities are very low (plasma almost absent) and the fluctuations very small;
- the plasmasheet (inside 14 R_s inbound and 12 R_s outbound), populated by high-energy particles (several tens of keV) with high intensities;
- the radiation belts (inside 10 R_s inbound and 8.5 R_s outbound), populated by very high-energy particles (0.1 to 1 MeV) with the highest intensities. Signatures of spatial (absorption by dust or icy satellites) and temporal (injection events) dynamics are observed in this region.

Although the inner and outer boundaries of the plasmasheet appear very well-marked (abrupt transitions) on Figure 2, *Krimigis et al.* reported frequent brief entry/exit (into the lobes) into a similar region during most of the outbound pass, characteristic of an extended and dynamic plasmasheet, with plasma motions off the equatorial plane.

2) The magnetometer data (panel 3 of Figure 2) have been used to characterize the magnetospheric regions by looking at large-scale changes in the field magnitude, orientation, and fluctuations [*Dougherty et al.*, 2005] and estimating the main contributions (internal and external) to the total magnetospheric field. The relative importance of each of these contributions enabled *Dougherty et al.* to distinguish three distinct regions both on the inbound and outbound passes:

- the lobe-like outer regions, where the contribution from the confinement of the magnetosphere by the solar wind to the total magnetospheric field is significant. In this region, the level of magnetic fluctuations appears very weak;

• the plasmasheet (inside 15 R_s inbound and 12 R_s outbound), where plasma effects inside the magnetosphere significantly contribute to the total magnetospheric field. In this region, the magnetic configuration is changing (the magnetic field lines are stretched) and is dominated by the radial component B_r. Moreover, the level of magnetic fluctuations is enhanced;

• the quasi-dipolar inner region (inside 5 R_s), where the contribution to the total magnetospheric field is dominated by the planetary intrinsic magnetic field. In this region, the magnetic field appears very steady and is dominated by the dipolar component B_θ.

3) Observations of large-scale changes in bulk properties and composition of the low-energy electron (panel 4 of Figure 2) and ion (panel 5 of Figure 2) plasma enabled *Young et al.* [2005] to distinguish three distinct regions both on the inbound and outbound passes:

• the high-latitude magnetosphere, where the low-energy plasma is almost absent and is composed mainly of protons due to the distance from the equatorial plane where heavier ions are more concentrated because of their higher masses;

• the outer plasmasphere (inside 14.4 R_s inbound and 13.6 R_s outbound), where the plasma contains a mixture of protons and water-group heavy ions, and is more variable. Both the protons and the water-group ions are observed to have energies close to the corotational temperatures (hence proportional to their mass, giving rise to the two proportional profiles evident in the fifth panel of Figure 2);

• the inner plasmasphere (inside 9 R_s inbound and 7.6 R_s outbound), where the plasma approximately corotates, is dominated by water-group ions and contains two electron components with temperatures of a few tens of eV and a few hundreds of eV. In particular, the A and B rings were observed to have an oxygen-rich atmosphere.

The transition from the high-latitude magnetosphere to the outer plasmasphere is characterized by an abrupt increase in plasma density.

4) The morphology of the magnetosphere has been identified with the help of the RPWS instrument (panel 6 of Figure 2) by looking at various plasma waves inside the magnetospheric cavity [*Gurnett et al.*, 2005]. These features enabled these authors to distinguish two main distinct regions both on the inbound and outbound passes:

- the relatively empty magnetosphere, where, in particular, the electrostatic band at the upper hybrid frequency (fuh) becomes undetectable;

- the dense and noisy inner magnetosphere (inside of about ∼10 R_s), where the strongest and most complex wave emissions are observed (electrostatic oscillations at the upper hybrid frequency, electron cyclotron harmonic waves and whistler mode emissions related to pitch-angle scattering and loss of energetic radiation belts electrons, and auroral hiss-like emissions near Saturn's rings). These plasma waves are in-situ and, therefore, exclude the SKR, dominant on panel 6 but which is a propagating radio emissions detected remotely. Finally, a systematic increase of electron densities (deduced from upper hybrid frequency emissions) with decreasing radial distances was observed, peaking near the outer edge of the planetary A ring.

This section identifies the different boundaries - and boundary names - at different locations, seen by different instruments. Using the characteristics of the different regions observed individually by the MAPS instruments, we can merge their description into four different regions and subregions, as marked by the vertical lines in Figure 2. As we will describe in section 8, these regions consist of the Saturnian ring system (Region 1, inside the dotted lines) and the cold plasma torus (Region 2, between the dotted and dashed lines) in the inner magnetosphere, the dynamic (between the dash-dotted and dashed lines) and extended (between the solid and dash-dotted lines) plasmasheet (Region 3), and the high-latitude outer magnetosphere (Region 4, outside the solid lines).

The inner magnetosphere is characterized by the presence of the dominant plasma and neutral sources of the Saturnian system, giving birth to a magnetosphere dominated by water group particles. The dynamic and extended plasmasheet, where the ring current resides, is a variable region with stretched magnetic field lines and contains a mixture of cold and hot plasma populations. The high-latitude outer magnetosphere is characterized by a very quiet magnetic field and an absence of plasma.

7. COMPARISON WITH VOYAGER

In order to compare the large-scale morphology of the Saturnian magnetosphere identified at the time of Voyager with the new picture observed by Cassini, we have superimposed on *Sittler et al.* [1983] original illustration the CAPS ELS and IMS measurements along the Cassini SOI inbound trajectory. Figure 3 provides us with the resulting picture. The regions crossed by the Cassini spacecraft during its SOI orbit do not differ drastically from what was previously observed by the Voyager spacecraft 23 years ago. The new CAPS measurements match the Voyager picture at noon remarkably, the same regions being qualitatively observed at equivalent radial and latitudinal distances.

A similar comparison can be done with observations from the magnetometers, energetic particle, and plasma wave instruments carried by Voyager and Cassini. We shall make use of published figures (in *Blanc et al.* [2002] and in the Cassini special issue of *Science*, volume *307*, 2005) in order to compare and contrast these observations.

We can first look at magnetic field residuals (i.e., when the contribution of the intrinsic planetary magnetic field [*Davis and Smith*, 1992] has been removed from original observations) from Voyager 1 and Cassini SOI inbound and outbound observations, in order to emphasize the effects associated with external magnetic field contributions (which include local plasma effects). *Dougherty et al.* [2005] reported that there indeed has been no noticeable change in the internal magnetic field between the two epochs, either in strength or in its near-alignment with the planetary rotation axis. In the inner magnetosphere, the largest contribution to the external magnetospheric field is from the ring current, up to 20-30 nT in magnitude. Using *Connerney et al.*'s [1983] azimuthaly symmetric ring current model, we can estimate the properties of this current system. *Dougherty et al.* [2005] indicated that the ring current within the magnetosphere was thinner (half-thickness $<$ 2 R_s) and more extended (inner radius $\sim$6 R_s and outer radius $>$ 20 R_s) than estimated at the time of Voyager (half thickness of 3 R_s, inner radius at 8 R_s, outer radius at 15.5 R_s). Values determined by *Bunce et al.* [2005] (albeit restricted to Cassini outbound SOI observations only) were 1.75 R_s, 6.5 R_s and 17.5 R_s, respectively. *Alexeev et al.* [2006] suggested that the ring current magnetic moment increases with system size, Cassini inbound SOI corresponding to the most expanded state with a magnetic moment equals to 1.5 times the Voyager 1 value. Whereas spin-periodic oscillations of the magnetic field were not discussed in the initial results of Cassini (cf. *Dougherty et al.*, [2005]), they were clearly present in retrospect [*Giampieri et al.*, 2006], as observed by previous spacecraft.

We can then look at LECP and MIMI LEMMS ion (> 30 keV) energy-time spectrograms for the complete Voyager 2 (Figure 3 in *Blanc et al.* [2002]) and Cassini SOI (Figure 1 of *Krimigis et al.*, [2005]) encounters. Remember that Voyager 2 closest approach occurred at a radial distance of 2.67 R_s, i.e. avoiding the main planetary ring system, contrary to Cassini. A first look at observations in the inner magnetosphere reveals that particle intensities are very similar for the two epochs, as well as their radial variations. Particularly noticeable in both spectrograms are a depletion in the intensity of energetic ions between the orbits of Dione and Enceladus, and an increase inside the orbits of Enceladus and Mimas [*Krimigis et al.*, 2005]. Finally, outbound observations reveal the large-scale dynamics of the Saturnian outer magnetosphere, with frequent entry/exit within lobe-like and plasmasheet-like regions.

We can finally look at the Planetary Radio Astronomy (PRA), Plasma Wave System (PWS) and RPWS frequency-time spectrograms for the Voyager 1 (Figure 18 in *Blanc et al.*, [2002]) and Cassini SOI (Figure 3 of *Gurnett et al.*, [2005]) encounters. The RPWS range indeed covers the PWS range and a large part of the PRA one. The most striking feature emerging from this comparison is undoubtedly the better temporal and frequency resolution of the RPWS instrument on-board Cassini, which provides much more detail than the PWS instrument (frequency range 10 Hz - 56 kHz) on-board Voyager (see for example the fine structures in the Saturn Kilometric Radiation reported by *Kurth et al.*, [2005b]). Finally, the most puzzling result reported by *Gurnett et al.* [2005] is the substantial shift (6 minutes) that has occurred in the radio rotation period between the Voyager (10 hours, 39 minutes, 24 $\pm$7 seconds) and Cassini era (10 hours, 45 minutes, 45 $\pm$36 seconds). As mentioned before, Ulysses observations previously revealed that the radio rotation period is not constant, fluctuating with time [*Galopeau and Lecacheux*, 2000], the reasons for this real physical difference being not well-understood.

In summary, the direct comparison between Voyager and Cassini SOI observations made possible by their relatively close trajectories shows that the large-scale structure of Saturn's magnetosphere was qualitatively similar at the two epochs. However, the vast improvements of Cassini instruments over those of Voyager provide us with a wealth of more detailed information, including original information on plasma dynamics and composition inside the inner magnetospheric regions of Saturn. These features are discussed in the next section, which converges on a unified view of the different Cassini observations.

8. A MULTI-INSTRUMENTAL VIEW

From the comparison of the regions and boundaries observed by the different MAPS instruments, we were able to identify four different regions in the first Cassini crossing of Saturn's magnetosphere. Let us now have a closer look at the MAPS data, using all instruments simultaneously, to point out specific processes characterizing each of these regions. Figure 4, which is repeated from Figure 2, shows the specific features used for this analysis in each data set. The interested reader can find the detailed observations in the references given in the text.

8.1. The Ring System (Region 1, within 3 R_s)

This region, which extends between the dotted vertical lines in Figure 2, covers the main A and B rings, and the F and G rings. It is characterized by a strong coupling between plasma, dust, and ring particles. We concentrate on the environment of the main rings: the unique data set returned by MAPS instruments in this region is shown in Figure 5, superposed on a visible image of a radial profile of the main rings structure provided by the ISS narrow-angle camera in October 2004. From left to right, one can see the B ring outer edge, the Cassini Division, and then the A ring with the Encke gap near its outer edge. Vertical lines are drawn to show the boundaries of the different regions, as well as the keplerian synchronous orbit near 1.85 R_s. Analysis of the MAPS instrument data sets over the rings reveals several interesting features.

Energetic particles. The main rings are a very strong absorber of energetic particles (observation 3 in panels 1 and 2 of Figure 4). The MIMI energetic particle fluxes drop below the measurement threshold exactly at the outer edge of the A ring, and no significant energetic particle flux is detected over the main rings. So the radiation belts stop exactly at the outer edge of the main rings. A second radiation belt, inside the main rings, planetward of the D ring, has been discovered by remote sensing using the INCA sensor which detected the energetic neutrals produced by this second belt [e.g., *Krimigis et al.*, 2005]. The main rings dig an empty cavity inside Saturn's radiation belts, in which production of neutrals and plasma can be due only to UV and low-energy particle irradiation, and to micro-meteorite bombardment of the ring particles. This production is important enough to maintain an exosphere and a tenuous ionosphere, which have been probed by the CAPS and INMS instruments and display specific chemical and dynamical features.

Structure of the ring ionosphere. The physical and dynamical structure of the rings has a direct imprint on the radial distribution of this ring ionosphere. The fluxes of low energy electrons seen by CAPS ELS (observation 2 in panel 4 of Figure 4) on the shaded side of the rings are directly anti-correlated with their optical thickness (bottom panel of Figure 5). This suggests a primary photo-production of electrons by UV photons on the sunlit side of the rings, opposite the spacecraft, followed by partial electron transmission through the ring plane [*Coates et al.*, 2004]. Electron fluxes reach their highest values inside the Cassini and Encke divisions. The ion population is also apparently influenced by the rings (observation 1 in panel 5 of Figure 4), though in a different way. CAPS IMS estimated densities are shown in Figure 5 [from *Tokar et al.*, 2005], for the two dominant ions O^+ (blue line) and ${O_2}^+$ (red line), together with the CAPS estimate of the total ion density (green line). The total electron density derived from RPWS plasma waves (black line) is also shown for comparison. No clear signature of the Cassini division is seen; but ion fluxes drop abruptly near the synchronous orbit at $\sim$1.85 R_s, suggesting that this may be the dominant effect. The average ion energy closely follows the value expected for local production of ions by pick-up from the rings neutral exosphere source [*Tokar et al.*, 2005]. This relationship of the plasma structure and dynamics to ring dynamics is also suggested by the RPWS electric field spectrogram taken in the same region (cf. Figure 5). One of its main features is the broad V-shaped emission centered on about 0330 UT with well defined low- and high-frequency cut-offs (causing its V-shape in the frequency-time plane) ranging from about 1 to 8 kHz. The V-shaped frequency-time variation of this emission is very similar to a commonly occurring terrestrial whistler-mode emission called auroral hiss. At Earth, auroral hiss is generated by magnetic field-aligned beams of low energy electrons (100 eV to several keV) associated with the current system responsible for the aurora. Similarly, the auroral hiss-like emissions observed near Saturn's rings strongly suggests that a low energy beam of electrons is being accelerated outward away from the ring at a radial distance of about 1.7 R_s, e.g. not far from the Keplerian synchronous orbit. Most likely this electron beam is associated with a current system induced by an electrodynamic interaction between the rings and the co-rotating magnetospheric plasma [*Gurnett et al.*, 2005; *Xin et al.*, 2006].

Chemical composition of the rings ionosphere. Two instruments, CAPS and INMS, were able to measure ion composition over the rings. Over the main rings, the CAPS IMS instrument detected the presence of atomic and molecular oxygen ions in the thermal plasma, as already pointed out. The Ion and Neutral Mass Spectrometer (INMS) found signatures of O^+, ${O_2}^+$, and H^+ ions [*Waite et al.*, 2005]. These measurements must be related to the potential ion sources. There are essentially two potential sources for the ring exosphere and ionosphere: (1) ultraviolet photo-dissociation of water vapour produced by meteoritic bombardment and (2) sputtering of the icy ring particles by photons or energetic particles. In the absence of energetic particles over the main rings, the ring ionosphere is likely to originate from ultraviolet photo-sputtering of the icy rings, producing free oxygen molecules and subsequent photo-ionization of O_2 [*Tokar et al.*, 2005]. But the absolute value of this source still needs to be assessed, with the possible use of test particle models [*Bouhram et al.*, 2006; *Luhmann et al.*, 2006].

Outside of the main rings, in the vicinity of the F and G rings, sputtering by energetic particles can be a more efficient source for the thermal plasma. The CAPS ELS instrument (observation 4 on panel 4 of Figure 4) observed a large nearly isotropic signal likely due to the penetration of high-energy particles from the trapped radiation belts. In these regions, dust impacts have been recorded by RPWS (*Wang et al.*, [2006], observation 5 on panel 6 of Figure 4).

8.2. The Cold Plasma Torus (Region 2, within 5-6 R_s)

This region, which extends between the dotted and dashed vertical lines in Figure 2, hosts the majority of the important sources of cold plasma, neutrals (the icy satellites Mimas, Tethys, Enceladus, and Dione), and dust (the diffuse E-ring). Its ion composition appears to be dominated by water-derived products. Neutrals have been known to be dominant there before Cassini observations, and to be chemically coupled to the multi-ion cold plasma [e.g., *Richardson*, 1998]. This cold plasma, being confined near the equatorial plane by the centrifugal force, gives rise to a corotating torus.

Electron density structure. From observations at the upper hybrid frequency and from quasi-thermal noise spectroscopy, *Gurnett et al.* [2005] and *Moncuquet et al.* [2005] determined plasma densities and temperatures. The local plasma density was found to increase continuously with decreasing radial distance (maximum at 170 cm^{-3} during the equatorial ring plane crossings), whereas the opposite prevailed for core electron temperatures (0.5 eV at 2.5 R_s to 6 eV at 6 R_s). Taking advantage of the excursion in latitude provided by the spacecraft trajectory, *Moncuquet et al.* [2005] evaluated the total plasma density in the equatorial plane and the plasma scale height, which appears to be very low just outside the main rings (0.1 R_s) and to increase rapidly with increasing radial distance (up to 0.9 R_s around 6 R_s).

Ion densities and composition. Cassini plasma instruments have the ability to resolve plasma composition and differentiate amongst the different water products, both at low energies (through CAPS IMS) and at high energies (through MIMI CHEMS). *Sittler et al.* [2005, 2006a] derived proton and water-group ion fluid moments using the CAPS IMS sensor. Their analysis was limited to inbound observations since the viewing of the corotation flow was not optimal on the outbound pass (noticeable in panel 5 of Figure 2, with reduced counts outbound). Water group ions are found to outnumber protons inside of Dione's orbit (observation 6 in panel 5 of Figure 4). Their temperatures decrease with decreasing radial distance (100 eV near the orbit of Rhea, 40 eV outside of Mimas orbit). CAPS data suggest the plasma flow is near the corotation speed inside the orbit of Dione, whereas *Wahlund et al.* [2005] derived azimuthal speeds significantly below co-rotation inside 5 R_s from RPWS Langmuir Probe observations. In fact, the Langmuir Probe saw two ion populations one - also observed by CAPS - moving at the corotation speed and one trapped near dust particles and moving at the Keplerian speed, the reported subcorotating azimuthal speeds being a weighted average of those two speeds. In addition, *Smith et al.* [2005] identified the presence of nitrogen ions in the inner magnetosphere using CAPS data. These ions have been detected at distances of 3.5-13.5 R_s from Saturn and at energies (< 2 keV) that indicate they are formed locally and not from inward diffusing Titan-generated plasma, otherwise they would be more energetic. Indeed, if they diffuse radially inward, while conserving the first and second adiabatic invariants, they can have energies greater than several hundred keV inside of Dione's orbit [*Sittler et al.*, 2006c]. The signal from these ions increases with decreasing distance from Saturn with the largest concentration of nitrogen ions detected near Enceladus' orbit. Thus, while some of these ions could originate from a Titan-generated neutral nitrogen torus, the dominate source appears to be at or near Enceladus [*Smith*, 2006].

The hot electron component (observations 8 on panel 1 of Figure 4 in MIMI LEMMS, but also noticeable in CAPS ELS data) drops significantly inside the inner torus where significant amounts of neutral oxygen have been observed [*Esposito et al.*, 2005]. More precisely, *Krimigis et al.* [2005] reported a depletion in the intensity of energetic ions and electrons between the orbits of Dione and Enceladus (panels 1 and 2 of Figure 2, between dashed lines, see the locations of the moons indicated on the Figure), followed by an increase inside the orbits of Enceladus and Mimas (starting just outside of the dotted lines, see the locations of the moons indicated on the Figure). The depletion of ions between the orbits of Dione and Enceladus suggest that the neutral gas observed by *Esposito et al.* [2005] may be the main sink for energetic particles through charge exchange.

8.3. The Dynamic and Extended Plasmasheet (Region 3, beyond 6 R_s)

This is the region located between the dashed and dash-dotted vertical lines in Figure 2, where we expect rotationally-driven and/or other modes of plasma transport to be important, as suggested by the many signatures of ion and electron dispersion seen by both CAPS and MIMI. It apparently extends outwards into a more tenuous plasma region, the extended plasma sheet (between dashed-dotted and solid lines). These regions are ideal to study how radial plasma transport processes can act to redistribute the magnetospheric plasma produced at different distances by a variety of sources. The mechanisms responsible for this transport are probably very diverse and seem to operate through different modes and on different scales as a function of radial distance [e.g., *Blanc et al.*, 2005]: fast neutral transport, radial plasma transport driven by small-scale or large-scale instabilities, or large-scale circulation cells. Among these mechanisms, flux tube interchange motions and the resulting localized particle dispersion events have been observed for the first time at Saturn by Cassini instruments.

Flux-tube interchange motions. The centrifugal instability (a Rayleigh-Taylor type instability with the centrifugal force playing the role of gravity) is known to trigger small-scale motions through the interchange of magnetic flux tubes [*Hill*, 1976]. SOI observations provided the first evidence that centrifugally-driven plasma motions take place in Saturn's corotation-dominated magnetosphere and contribute (at least partly) to plasma redistribution in the magnetospheric system: several of the observed magnetic field and plasma signatures can be related to plasma transport triggered by the interchange instability [*André et al.*, 2005; *Burch et al.*, 2005; *Hill et al.*, 2005; *Leisner et al.*, 2005; *Mauk et al.*, 2005]. Through this process magnetic flux tubes of dense and cold plasma move outwards and are replaced by flux tubes of tenuous and hot plasma that return inwards.

Between 6 and 10 R_s (observation 9 on panel 3 of Figure 4), the MAG instrument reported numerous observations of localized magnetic flux tubes in which a decrease of the magnetic pressure is balanced by increased plasma pressure. These flux tubes, of large duration and size, appeared more dipolar than their surroundings, an effect associated with the reduced efficiency of the centrifugal force in stretching the magnetic field lines since their plasma mass content is probably lower [*Leisner et al.*, 2005]. RPWS observations of the local total plasma density inside these flux tubes (from the upper hybrid frequency) confirmed the presence of a density cavity within these flux tubes (observation 10 on panel 6 of Figure 4).

Associated particle dispersion events. The CAPS and MIMI instruments revealed localized planetward injections of hot ion and electron plasma (in the tens to hundreds of keV range) between 4 and 11 R_s (observations 11 on panels 4 and 5 of Figure 4). These energy-time dispersed signatures are produced by the combination of localized inward transport of hot plasma and azimuthal, energy-dependent gradient and curvature drifts. The injections responsible for these signatures appear to be randomly distributed in local time and Saturnian longitude [*Hill et al.*, 2005], as we expect for a rotationally-driven transport process. *Burch et al.* [2005] modelled CAPS observations of drift dispersion signatures occurring within an interchanging flux tube that penetrated deep into the magnetosphere, bringing with it a density cavity and hot plasma, both characteristic of the environment observed at larger distances. Interestingly, *Mauk et al.* [2005] pointed out similarities with hot plasma injection signatures at Jupiter [*Mauk et al.*, 1999]. In addition, this region is further fully pervaded by a two-component electron population, similarly to what *Frank and Paterson* [2000] observed in the Io torus.

Figure 6 summarizes observations from RPWS, CAPS ELS and IMS, and MAG of an interchange event observed on June 30 around 21:05 UT. A detailed examination of this figure reveals the presence of an isolated magnetic flux tube (between vertical brown lines) with unusual plasma and magnetic properties. This flux tube is observed at a radial distance of $R = 5.94$ R$_s$ and at a distance of $Z = 1$ R$_s$ below the magnetospheric equatorial plane. This flux tube is characterized by the following properties:

1. it contains less plasma than its surroundings, as deduced from the observation of the slight (by a factor 2) decreases of the upper hybrid frequency (first panel of Figure 6);

2. it is associated with an hotter electron population (second panel of Figure 6). This suprathermal electrons may be produced locally by field-aligned currents or accelerated in the outer magnetosphere and transported inwards. *Rymer et al.*, [2007] identified the likely source of this hotter electron population to be the middle magnetosphere, with transport

to the inner magnetosphere via radial diffusion regulated by discrete interchange-like injections as observed in the particular flux tube discussed here;

3. it is depleted of its cold plasma content, as deduced from the observation of noticeable gaps in the water-group ions and protons energy bands appearing in the IMS spectrogram (third panel of Figure 6);

4. the magnetic pressure of this flux tube is depressed compared to its surroundings (fourth panel of Figure 6). It appears more dipolar than its surroundings (sixth panel of Figure 6, because it contains less plasma and thus has a lower centrifugal stress (*Leisner et al.* [2005]).

In summary, these first Cassini observations of interchange events at Saturn opens the way for comparative studies between the Jovian and Saturnian environments, likely to improve our understanding of the interchange instability and to complement previous Galileo observations at Jupiter.

8.4. The Outer High-Latitude Magnetosphere (Region 4, beyond 12-14 R_s)

Observations taken in this region, which extend outside the solid vertical lines in Figure 2, are of limited use due to the high-latitude location of the spacecraft and the scarcity of particle populations there, the spacecraft was likely outside of the plasmasheet and inside the lobes. More interesting observations in this region have been reported after July 1, 2004: *Krimigis et al.* [2005] and *Krupp et al.* [2005] reported frequent brief entry/exit in lobe-like and plasmasheet-like regions during the outbound pass, suggesting an extended and very dynamic plasmasheet. *Louarn et al.* [2004] described 50-90 minutes modulations of whistler mode waves around 50 Hz observed by RPWS (observation 12 on panel 6 of Figure 4) and correlated them with fluxes of auroral radio emissions (remote observations) and of energetic particles (in-situ observations). They suggested that global scale magnetospheric oscillations are part of the activity of Saturn's magnetosphere. *Bunce et al.* [2005] reported on the outbound pass what could be an evidence of tail collapse via magnetic reconnection and hot plasma acceleration in Saturn's magnetotail that may be related to a compression of the magnetosphere by a corotating interaction region (CIR). These compressions have been recently suggested by *Cowley et al.* [2005] (reconnection model) and *Sittler et al.* [2006b] (centrifugal instability model) to be important drivers of Saturn's auroral dynamics. So, despite the limits inherent to single-point measurements and to a very tenuous plasma, measurements in this region of the outer magnetosphere will be very useful to monitor large-scale dynamical events in Saturn's magnetosphere.

9. PLASMA PROCESSES

At the end of the year 2007, Cassini has already been orbiting Saturn 57 times. The Cassini spacecraft has not yet returned to the ring magnetosphere, and, as a consequence, SOI provided us with unique in-situ observations of the ring environment. Whereas it was not possible to use SOI observations in order to address the exact role played by Titan and its dense atmosphere in Saturn's magnetosphere, other orbits will enable us to investigate this issue in details, having flown by the moon 40 times at the end of 2007. Since 2004, additional campaigns of solar wind measurements by Cassini and auroral observations by HST were coordinated and will enable to further diagnose the dynamics of the Saturnian magnetosphere in order to identify and quantify the respective importance of the solar wind and planetary rotation drivers. All these different pieces will have in the future to be merged and properly added to our description, as soon as all MAPS and related data will have been examined in common, as done during SOI.

We shall focus our attention on the three pre-Cassini issues identified in section 2 and show how new Cassini observations enabled us to unveil part of their mysteries and stimulate intense ongoing research activities.

9.1. Magnetospheric Mass-Loading

SOI observations confirmed that the mass loading of the system occurs deep inside the magnetosphere, in regions where the icy moons Mimas, Enceladus, Tethys, Dione, Rhea, and E-ring particles are orbiting, and known to be host to various dust, neutral, and plasma sources. Later, data from more equatorial orbits [*Persoon et al.*, 2005] gave further evidence that the dominant and variable contribution to the magnetospheric plasma is located inside 5 R_s. Whereas several past observations pointed out the peculiar role played by Enceladus in the Saturn's system, the dramatic nature of this activity has now been clearly identified. The flybys of Enceladus in 2005 led to the discovery, first revealed by one of the MAPS instrument (MAG), of the significant contribution of this moon in supplying plumes of freshly created water-group ions through charge exchange and impact ionization of water ice and dust particles ejected from its south polar region [*Dougherty et al.*, 2006; *Spahn et al.*, 2006; *Tokar et al.*, 2006; *Hansen et al.*, 2006]. Compositional data from INMS indicated that the atmospheric plume is dominated by water, with nonnegligible amount of carbon dioxide, carbon monoxide or molecular nitrogen, and methane [*Waite et al.*, 2006]. CAPS IMS data indicated that H_3O^+ is a major ion near Enceladus [*Tokar et al.*, 2006]. These species were, however, not included in plasma transport and chemistry models [*Richardson and Jurac*, 2005] that remain to be updated.

The discovery by Cassini of an unexpected ongoing geological activity at Enceladus provides the solution for the missing neutral water source, the replenishing of E-ring particles, and the larger neutral source rate required by the models built after the Voyager encounters [*Richardson*, 1998]. From the new Cassini observations, *Johnson et al.* [2006] proposed that the venting of water produces a narrow torus of, primarily, undissociated water around Enceladus and that charge-exchange collisions in this narrow torus between corotating ions and neutrals then populate the broad neutral torus observed by UVIS during the approach phase, as well as by HST in the past. *Burger et al.* [2007] estimated that Enceladus emits 300 kg (10^{28} water molecules)/s - a similar rate being inferred from UVIS stellar occultation data at Enceladus [*Hansen et al.*, 2006] - as required by pre-Cassini models. This produces 3 kg/s of fresh water group ions [*Burger et al.*, 2007], consistent with estimates of the mass loading rate inferred from MAG observations [*Khurana et al.*, 2007]. Enceladus is revealing itself to be an important plasma source at Saturn, perhaps, analogously, albeit on a smaller scale, to Io at Jupiter. Ion cyclotron wave activity generated by the pick up water group ions freshly created has been found throughout Saturn's E ring out to 6-7 R_s, both near and far from the icy moons. These observations give us further insights into the mass-loading process [*Leisner et al.*, 2006].

Not only magnetospheric scientists were amazed that this tiny moon is so active, venting water vapor, dust and plasma from localized fractures ('tiger stripes') within regions of high heat flux near its south pole [*Porco et al.*, 2006; *Spencer et al.*, 2006; *Hansen et al.*, 2006; *Spahn et al.*, 2006]. The plume characteristics and the surprisingly high temperatures make it likely that Enceladus has a subsurface ocean, either global or possibly localized, beneath a thick ice shell [*Nimmo et al*, 2007]. The discovery of the activity of the moon raises many questions on the energy sources that powers this activity and, hence, on the formation of the Saturn system. Together with the Jovian moon Europa, Enceladus may therefore present an additional opportunity for the detection of extant life in our solar system [*Parkinson et al.*, 2007] which makes the study of the composition of the plumes particularly important. The next very close flyby of the moon, expected in March 2008, will bring scientists with new surprises. But, at the moment, it is clear to everybody that it is only by means of global and pluridisciplinary studies that we will gain a better and complete understanding of this fascinating planetary body.

9.2. Radial Transport

SOI observations enabled first in-situ inspection of some consequences of the internal mass-loading on the dynamics of Saturn's magnetosphere. Later orbits confirmed the dynamic state of the extended plasmasheet, where signatures of interchanging flux tubes and associated plasma injection events are observed to be prevalent inside 11 R_s. The centrifugal force is therefore a driver of important dynamical phenomena for the plasma locally created. This region is further fully pervaded by a two-component electron population (a cold one, 1-100 eV and a hotter one, 1-100 keV). The source of the former was shown to be distributed in the region, whereas that of the latter was found consistent with inward plasma transport from the outer magnetosphere [*Rymer et al.*, 2006]. The plasma transport was suggested to be slow enough so that the cold electrons can equilibrate with the ions through Coulomb collisions.

So far the rotationally-driven plasma circulation in the Saturnian magnetosphere appears to be very similar to the plasma circulation in the Jovian magnetosphere [*Krupp et al.* [2004]; *Russell*, 2000, 2001]. Inward plasma transport occurs in localized events, characterized by plasma-depleted flux tubes associated with hot plasma injections. Outward plasma transport does not take the form of such discrete isolated events, and, on the contrary, recent evidence exists for this transport being consistent with a general plasma outflow [*Burch et al.*, 2007] based on CAPS ELS observations of butterfly electron pitch-angle distributions in the background plasma. *Burch et al.* [2007] further demonstrated that these distributions result from the transport of plasma from regions near the orbits of Dione (6.26 R_s) and Tethys (4.88 R_s), suggesting the presence of distinct plasma tori associated with these moons. The observed plasma-depleted flux tubes participate in the overall cycle of outward/inward plasma transport by returning planetwards the magnetic flux carried outwards by denser flux tubes. These denser flux tubes must lose their plasma content at some location in the magnetosphere. This may be the result from the breaking of flux tubes in the near tail on the nightside of the magnetosphere [*Curtis et al.*, 1986; *Sittler et al.*, 2006b]. Recent Cassini measurements between 40 and 50 R_s downtail revealed strong, rapid dipolarizations of the magnetic field, signalling the episodic release of energy to the magnetosphere and plasma to the solar wind [*Jackman et al.*, 2007]. The observations reported were similar in a sense to those seen at Jupiter [*Russell et al.*, 1998], but also with terrestrial substorms, with the fast planetary rotation adding phenomenology not seen at Earth [*Mitchell et al.*, 2005] where the effects of external conditions prevail.

In short, various processes may contribute to the radial plasma transport in the Saturnian magnetosphere. All these processes trigger variations in the transport rate of the plasma and its radial redistribution. The chain of processes involved in the exchanges of momentum and the dissipation of rotational energy in this huge system is complex. As all objects in the solar system, Saturn interacts with the solar wind which drives a part of the magnetospheric dynamics and possibly triggers major storms when solar perturbations hit the magnetosphere. Determining the spatial/temporal scales of these processes, quantifying their relative efficiency and how they vary with the activity of Enceladus remain to be properly assessed, as well as the question concerning the respective importance of external and internal processes in the regulation of the activity of this magnetic environment.

9.3. Rotational Modulation

Cassini observations during later orbits further demonstrated that planetary spin-periodic perturbations in all field and particle observations are ubiquituous in the whole Saturn's magnetosphere. Images of the ring current at Saturn, based on MIMI measurements, revealed an highly variable ring current with strong longitudinal asymmetries that corotate nearly rigidly with the planet [*Krimigis et al.*, 2007]. Planetary-period oscillations of the radial and azimuthal magnetic field components are always present in the quasi-dipolar regions of Saturn's magnetosphere, whereas compressional oscillations in the radial component are dominant in tail-like regions [*Cowley et al.*, 2006]. Magnetopause boundary oscillations at the planetary period also commonly occur, which are in phase with the plasma pressure variations inside the magnetosphere [*Clarke et al.*, 2006]. These observations are consistent with a Camshaft model [*Espinosa et al.*, 2003b] in which a compressive wave originates from a corotating source (the cam) in the nearer-planet region and propagates outward through the sub-corotating outer magnetospheric plasma. *Southwood and Kivelson* [2007] discussed a system of field-aligned currents which produce the observed cam field in the inner magnetosphere and produce an effective dipole tilt in the outer magnetosphere which produces the outer magnetospheric periodicities. *Carbary et al.* [2007] proposed that the compression/expansion action of the cam in the inner magnetosphere effectively shakes the outer magnetosphere, which is tilted ∼20 degrees relative to the solar wind flow, and produces tailward-moving transverse waves in synchrony with the rotation of the inner magnetosphere that cause the observed periodicities. *Gurnett et al.* [2007] recently reported the occurence of a rotational modulation of the plasma density and magnetic field near the orbit of Enceladus that is phase-locked to the time-variable SKR modulation [*Kurth et al.*, 2006] and proposed that a two-cell corotating convection pattern with stronger centrifugally-driven plasma outflow on its dense side acts as the cam. This centrifugally driven convection can spontaneously break the axisymmetry of the external magnetic field at Saturn [*Goldreich and Farmer*, 2007] and drive other planetary-period modulated magnetospheric effects such as the SKR. The dynamics of Saturn magnetosphere may, therefore, be dominated by responses to plasma introduced by Enceladus [*Kivelson*, 2006] but the true picture may probably be more complex, involving external influence as well. *Cecconi and Zarka* [2005] proposed for example that variations of solar wind characteristics at Saturn, especially its velocity, result in a displacement of the radio sources in local time and modify the apparent SKR radio period. Zarka et al. [2007] reported that SKR period varies systematically by $\pm 1\%$ with a characteristic timescale of 20-30 days. These fluctuations were found to correlate with solar wind speed at Saturn. Therefore, nonrandom fluctuations in the solar wind speed at Saturn can cause SKR source displacement in local time, leading to an apparent radio period that is different from the planet's true rotation period.

All the models constructed to explain the observed plasma and field periodicities have largely been constructed to explain the behaviour of a single dataset and, hence, are not yet complete. Once combined, Cassini multi-instrument observations should gradually unveil all these enigmas. Identifying the mechanism behind this periodic modulation is a prime goal of Cassini magnetospheric scientists. In addition, Saturn's rotational rate is a fundamental parameter for atmospheric, magnetospheric, and interior studies of the planet [*Sanchez-Lavega*, 2005]. Determination of a definitive, fixed rotation period is therefore a high priority for most planetary scientists. Since Saturn lacks a solid surface, determining the planetary rotation period is difficult. Measuring the motions of features on the atmosphere can also lead to inaccuracies due to atmospheric wind speeds. Tracking the rotational modulation of the radio emissions SKR (linked to the planetary field, which originates in the interior of the planet) over a long-period of time could therefore provide the most accurate answer in the future.

10. SUMMARY

The present observational review article focuses on the identification of Saturn's magnetospheric regions and associated plasma processes, based on the very first orbit of the Cassini-Huygens spacecraft around the planet. Our objective is to illustrate to the general planetary communities how to extract scientific information from the observations obtained by the particle and field instruments onboard Cassini. SOI observations enabled us to capture a snapshot of the large-scale structure of the Saturnian magnetosphere and of some of the main plasma processes operating in this complex environment. We combined all different observations in a coordinated manner, in order to gain a deeper understanding of the Saturnian system.

Remote sensing observations of Saturn's magnetosphere during the approach phase confirmed Voyager's evidence for a double control of the auroral and radio emissions by the solar wind and by the planetary rotation. It also showed that the magnetosphere is immersed to large distances in a neutral gas cloud with densities comparable to or larger than the plasma densities, and that its strong corotation electric field accelerated Saturnian dust particles into interplanetary space.

During Saturn Orbit Insertion, in situ observations by the MAPS instruments provided the first Cassini cross-section across the main magnetospheric regions of the Saturnian system. We basically identified similar regions to those identified previously by Voyager, though with a much more powerful measurements capability. From its innermost regions to the magnetopause, four different plasma domains could be identified:

- the ring system (Region 1), conjugate to the main rings inside 3 R_s, is populated by plasma produced by UV sputtering of the sunlit side of the rings, and dominated by oxygen ions which follow corotation. It is essentially void of energetic particles due to ring absorption. This region is characterized by strong coupling between plasma, gas and ring particles.

- the cold plasma torus (Region 2) is a region dominated by co-rotating water products with essentially no evidence of suprathermal electron or ion population. It extends to approximately 5 to 6 Rs outside. Plasma supply via pick-up of ions and charge exchange are key processes operating in this region, in order to explain the observed density gradient and the depletion of energetic particles.

- beyond this orbit, the dynamic and extended plasmasheet (Region 3) is populated by the same low-energy plasma upon which a spatially structured population of suprathermal electrons is superimposed. The numerous signatures of flux-tube interchange and associated particle energy dispersion reveal the importance of radial plasma transport in this region.

• finally, beyond a relatively sharp outer edge, Cassini probed the outer high-latitude magnetosphere (Region 4), in which the plasma is very tenuous and particle measurements difficult, but observations suggest this region is more dynamic than initially thought.

The preliminary identification of the magnetospheric regions described in the present paper will have to be deepened and contrasted by the analysis of additional sets of Cassini orbits, and bring new constraints to previous and current models. Thanks to its broad coverage of Saturn's magnetosphere, Cassini-Huygens will make it possible to study a system which is in strong interaction with all other components of Saturn's environment. The analysis of the broad diversity of these interaction processes will be one of the main themes of Magnetospheric and Plasma Science during the Cassini mission. It will ultimately be possible to give a more complete and definitive overview of the time-variability and large-scale three-dimensional structure of Saturn's multi-faceted magnetosphere, as well as to elucidate many of the outstanding issues coming from these unique observations.

ACKNOWLEDGMENTS. The authors acknowledge the support of the Cassini Project and particularly all the MAPS instrumental teams for making of the Cassini mission such an outstanding success.

REFERENCES

Alexeev, I. I., V. V. Kalegaev, E. S. Belenkaya, S. Y. Bobrovnikov, E. J. Bunce, S. W. H. Cowley, and J. D. Nichols (2006), A global magnetic model of Saturn's magnetosphere and a comparison with Cassini SOI data, *Geophys. Res. Lett., 33*, L08101, doi:10.1029/2006GL025896.

André, N., M. K. Dougherty, C. T. Russell, J. S. Leisner, and K. K. Khurana (2005), Dynamics of Saturnian inner magnetosphere: First inferences from the Cassini magnetometers about small-scale plasma transport in the magnetosphere, *Geophys. Res. Lett., 32*, L14S06, doi:10.1029/2005GL022643.

Arridge, C. S., N. Achilleos, M. K. Dougherty, K. K. Khurana, and C. T. Russell (2006), Modeling the size and shape of Saturn's magnetopause with variable dynamic pressure, *J. Geophys. Res., 111*, A11227, doi:10.1029/2005JA011574.

Belenkaya, E. S., S. W. H. Cowley, and I. I. Alexeev (2006), Saturn's aurora in the January 2004 events, *Ann. Geophys.*, *24*, 1649.

Blanc, M., S. Bolton, J. Bradley, M. E. Burton, T. E. Cravens, I. Dandouras, M. K. Dougherty, M. C. Festou, J. Feynman, R. E. Johnson, T. G. Gombosi, W. S. Kurth, P. C. Liewer, B. H. Mauk, S. Maurice, D. Mitchell, F. M. Neubauer, J. D. Richardson, D. E. Shemansky, E. C. Sittler, B. T. Tsurutani, P. Zarka, L. W. Esposito, E. Grün, D. A. Gurnett, A. J. Kliore, S. M. Krimigis, D. J. Southwood, J. H. Waite, and D. T. Young (2002), Magnetospheric and Plasma Science with Cassini-Huygens, *Space Sci. Rev.*, *104*, 253.

Blanc, M., R. Kallenbach, and N. V. Erkaev (2005), Solar System Magnetospheres, *Space Sci. Rev.*, *116*, 227-298.

Bolton, S. J., R. M. Thorne, D. A. Gurnett, W. S. Kurth, and D. J. Williams (1997), Enhanced whistler-mode emissions: Signatures of interchange motion in the Io torus, *Geophys. Res. Lett., 24*, 2123.

Bouhram, M., R. E. Johnson, J.-J. Berthelier, J.-M. Illiano, R. L. Tokar, D. T. Young, and F. J. Crary (2006), A test-particle model of the atmosphere/ionosphere system of Saturn's main rings, *Geophys. Res. Lett., 33*, L05106, doi:10.1029/2005GL025011.

Burch, J. L., J. Goldstein, T. W. Hill, D. T. Young, F. J. Crary, A. J. Coates, N. André, W. S. Kurth, and E. C. Sittler Jr. (2005), Properties of local plasma injections in Saturn's magnetosphere, *Geophys. Res. Lett., 32*, L14S02, doi:10.1029/2005GL022611.

Burch, J. L., J. Goldstein, W. S. Lewis, D. T. Young, A. J. Coates, M. K. Dougherty, and N. André (2007), Tethys and Dione: Sources of outward flowing plasma in Saturn's magnetosphere, *Nature*, *447*, doi:10.1038/nature05906.

Bunce, E. J., S. W. H. Cowley, D. M. Wright, A. J. Coates, M. K. Dougherty, N. Krupp, W. S. Kurth, and A. M. Rymer (2005), In situ observations of a solar wind compression-induced hot plasma injection in Saturn's tail, *Geophys. Res. Lett., 32*, L20S04, doi:10.1029/2005GL022888.

Burger, M. H., E. C. Sittler, R. E. Johnson, H. T. Smith, O. J. Tucker, and V. I. Shematovich (2007), Understanding the escape of water from Enceladus, *J. Geophys. Res., 112*, A06219, doi:10.1029/2006JA012086.

Carbary, J. F. and S. M. Krimigis (1982), Charged particle periodicity in Saturn's magnetosphere, *Geophys. Res. Lett., 9*, 1073.

Carbary, J. F., D. G. Mitchell, S. M. Krimigis, D. C. Hamilton, and N. Krupp (2007), Spin-period effects in magnetospheres with no axial tilt, *Geophys. Res. Lett., 34*, L18107, doi:10.1029/2007GL030483.

Cecconi, B., and P. Zarka (2005), Model of a variable radio period for Saturn, *J. Geophys. Res., 110*, A12203, doi:10.1029/2005JA011085.

Clarke, J. T., J.-C. Gérard, D. Grodent, S. Wannawichian, J. Gustin, J. Connerney, F. Crary, M. K. Dougherty, W. Kurth, S. W. H. Cowley, E. J. Bunce, T. Hill, and J. Kim (2005), Morphological differences between Saturn's ultraviolet aurorae and those of Earth and Jupiter, *Nature*, *433*, 717.

Clarke, K., E., N. André, D. J. Andrews, A. J. Coates, S. W. H. Cowley, M. K. Dougherty, G. R. Lewis, H. J. McAndrews, J. D. Nichols, T. R. Robinson, and D. M. wright (2006), Cassini observations of planetary-period oscillations of Saturn's magnetopause, *Geophys. Res. Lett., 33*, L23104, doi:10.1029/2006GL027821.

Coates, A. J., H. J. McAndrews, A. M. Rymer, D. T. Young, F. J. Crary, S. Maurice, R. E. Johnson, R. A. Baragiola, R. L. Tokar, E. C. Sittler, and G. R. Lewis (2005), Plasma electrons above Saturn's main rings: CAPS observations, *Geophys. Res. Lett., 32*, L14S09, doi:10.1029/2005GL022694.

Connerney, J. E. P., M. H. Acuna, and N. F. Ness (1983), Currents in Saturn's magnetosphere, *J. Geophys. Res., 88*, 8779.

Cowley, S. W. H., S. V. Badman, E. J. Bunce, J. T. CLarke, J.-C. Gérard, D. Grodent, C. M. Jackman, S. E. Milan, and T. K. Yeoman (2005), Reconnection in a rotation-dominated magnetosphere and its relation to Saturn's dynamics, *J. Geophys. Res., 110*, doi:10.1029/2005JA010796.

Cowley, S. W. H., D. M. Wright, E. J. Bunce, A. C. Carter, M. K. Dougherty, G. Giampieri, J. D. Nichols, and T. R. Robinson (2006), Cassini observations of planetary-period magnetic field oscillations in Saturn's magnetosphere: Doppler shifts and phase motion, *Geophys. Res. Lett., 33*, L07104, doi:10.1029/2005GL025522.

Crary, F. J., J. T. Clarke, M. K. Dougherty, P. G. Hanlon, K. C. Hansen, J. T. Steinberg, B. L. Barraclough, A. J. Coates, J.-C. Gérard, D. Grodent, W. S. Kurth, D. G. Mitchell, A. M. Rymer, and D. T. Young (2005), Solar wind dynamic pressure and electric field as the main factors controlling Saturn's aurorae, *Nature*, *433*, 720.

Curtis, S. A., R. P. Lepping, and E. C. Sittler (1986), the centrifugal flute instability and the generation of the Saturnian kilometric radiation, *J. Geophys. Res., 91*, 10,989-10,994.

Davis, L., Jr., and E. J. Smith (1992), A model of Saturn's magnetic field based on all available data, *J. Geophys. Res., 95*, 15,257.

Delamere, P. A., F. Bagenal, V. Dols, and L. C. Ray (2007), Saturn's neutral torus versus Jupiter's neutral torus, *Geophys. Res. Lett., 34*, L09105, doi:10.1029/2007GL029437.

Desch, M. D. and H. O. Rucker (1983), The relationship between Saturn kilometric radiation and the solar wind, *J. Geophys. Res., 88*, 8,999.

Dougherty, M. K., S. Kellock, D. J. Southwood, A. Balogh, E. J. Smith, B. T. Tsurutani, B. Gerlach, K.-H. Glassmeier, F. Gleim, C. T. Russell, G. Erdös, F. M. Neubauer, and S. W. H. Cowley (2004), The Cassini magnetic field investigation, *Space Sci. Rev.*, *114*, 331.

Dougherty, M. K., N. Achilleos, N. André, C. S. Arridge, A. Balogh, C. Bertucci, M. E. Burton, S. W. H. Cowley, G. Erdös, G. Giampieri, K.-H. Glassmeier, K. K. Khurana, J. S. Leisner, F. M. Neubauer, C. T. Russell, E. J. Smith, D. J. Southwood, and B. T. Tsurutani (2005), Cassini magnetometer observations during Saturn Orbit Insertion, *Science*, *307*, 1266.

Dougherty, M. K., K. K. Khurana, F. M. Neubauer, C. T. Russell, J. Saur, J. S. Leisner, and M. E. Burton. (2006), Identification of a dynamic atmosphere at Enceladus with the Cassini Magnetometer, *Science*, *311*, 1406.

Espinosa, S. A., D. J. Southwood, and M. K. Dougherty (2003a), Reanalysis of Saturn's magnetospheric field data view of spin-periodic perturbations, *J. Geophys. Res., 108*, 1085, doi:10.1029/2001JA005083.

Espinosa, S. A., D. J. Southwood, and M. K. Dougherty (2003b), How can Saturn impose its rotation period in a noncorotating magnetosphere ?, *J. Geophys. Res., 108*, 1086, doi:10.1029/2001JA005084.

Esposito, L. W., C. A. Barth, J. E. Colwell, G. M. Lawrence, W. E. McClintock, A. Stewart, F. Ian, H. U. Keller, A. Korth, H. Lauche, M. C. Festou, A. L. Lane, C. J. Hansen, J. N. Maki, R. A. West, H. Jahn, R. Reulke, K. Warlich, D. E. Shemansky, Y. L. Yung (2004), The Cassini Ultraviolet Imaging Spectrograph Investigation, *Space Sci. Rev.*, *114*, 299.

Esposito, L. W., J. E. Colwell, K. Larsen, W. E. McClintock, A. I. F. Stewart, J. T. Hallett, D. E. Shemansky, J. M. Ajello, C. J. Hansen, A. R. Hendrix, R. A. west, H. U. Keller, A. Korth, W. R. Pryor, R. Reulke, and Y. L. Yung (2005), Ultraviolet Imaging spectroscopy shows an active Saturnian system, *Science*, *307*, 1251.

Eviatar, A., G. L. Siscoe, J. D. Scudder, E. C. Sittler, and J. D. Sullivan, The plumes of Titan (1982), *J. Geophys. Res., 87*, 8091.

Frank, L. A., and W. R. Paterson (2000), Observations of plasmas in the Io torus with the Galileo spacecraft, *J. Geophys. Res., 105*, doi:10.1029/1999JA000250.

Galopeau, P. H. M., A. Ortega-Molina, and P. Zarka (1991), Evidence of Saturn's magnetic field anomaly from Saturnian kilometric radiation high-frequency limit, *J. Geophys. Res., 96*, 14,129-14,140.

Galopeau, P. H. M., P. Zarka, and D. Le Quéau (1995), Source location of Saturn's kilometric radiation: the Kelvin-Helmholtz instability hypothesis, *J. Geophys. Res., 100*, 26,397-26,410.

Galopeau, P. H. M. and A. Lecacheux (2000), Variations of Saturn's radio rotation period measured at kilometer wavelengths, *J. Geophys. Res., 105*, 13,089-13,102.

Giampieri, G., M. K. Dougherty, E. J. Smith, and C. T. Russell (2006), A regular period for Saturn's magnetic field that may track its internal rotation, *Nature*, *44*, doi:10.1038/nature04750.

Goertz, C. K. (1983), Detached plasma in Saturn's front side magnetosphere, *Geophys. Res. Lett., 10*, 455.

Goldreich, P. and A. J. Farmer (2007), Spontaneous axisymmetry breaking of the external magnetic field at Saturn, *J. Geophys. Res., 112*, A05225, doi:10.1029/2006JA012163.

Gurnett, D. A., W. S. Kurth, D. L. Kirchner, G. B. Hospodarsky, T. F. Averkamp, P. Zarka, A. Lecacheux, R. Manning, A. Roux, P. Canu, N. Cornilleau-Wehrlin, P. Galopeau, A. Meyer, R. Boström, G. Gustafsson, J.-E. Wahlund, L. Ahlen, H. O. Rucker, H. P. Ladreiter, W. Macher, L. J. C. Woolliscroft, H. Alleyne, M. L. Kaiser, M. D. Desch, W. M. Farrell, C. C. Harvey, P. Louarn, P. J. Kellogg, K. Goetz, and A. Pedersen (2004), The Cassini radio and plasma wave investigation, *Space Sci. Rev.*, *114*, 395.

Gurnett, D. A., W. S. Kurth, G. B. Hospodarsky, A. M. Persoon, T. F. Averkampf, B. Cecconi, A. Lecacheux, P. Zarka, P. Canu, N. Cornilleau-Wehrlin, P. Galopeau, A. Roux, C. Harvey, P. Louarn, R. Boström, G. Gustafsson, J.-E. Wahlund, M. D. Desch, W. M. Farrell, M. L. Kaiser, K. Goetz, P. J. Kellogg, G. Fischer, H.-P. Ladreiter, H. Rucker, H. Alleyne, and A. Pedersen (2005), Radio and Plasma Wave observations at Saturn: Initial results from Cassini, *Science*, *307*, 1255.

Gurnett, D. A., A. M. Persoon, W. S. Kurth, J. B. Groene, T. F. Averkamp, M. K. Dougherty, and D. J. Southwood (2007), The variable rotation period of the inner regions of Saturn's plasma disk, *Sci.*, *316*, 442-444.

Hansen, C. J., L. Esposito, A. I. F. Stewart, J. Colwell, A. Hendrix, W. Pryor, D. Shemansky, and R. West (2006), Enceladus' water vapor plume, *Sci.*, *311*, 1422-1425.

Hansen, K. C., A. J. Ridley, G. B. Hospodarsky, N. Achilleos, M. K. Dougherty, T. I. Gombosi, and G. Tóth (2005), Global MHD simulations of Saturn's magnetosphere at the time of Cassini approach, *Geophys. Res. Lett., 32*, L20S06, doi:10.1029/2005GL022835.

Hendricks, S., F. M. Neubauer, M. K. Dougherty, N. Achilleos, and C. T. Russell (2005), Variability in Saturn's bow shock and magnetopause from Pioneer and Voyager: Probabilistic predictions and initial observations by Cassini, *Geophys. Res. Lett., 32*, L20S08, doi:10.1029/2005GL022569.

Hill, T. W. (1976), Interchange instability of a rapidly rotating magnetosphere, *Planet. Space Sci., 24*, 1151.

Hill, T. W., A. M. Rymer, J. L. Burch, F. J. Crary, D. T. Young, M. F. Thomsen, D. Delapp, N. André, A. J. Coates, and G. R. Lewis (2005), Evidence for rotationally driven plasma transport in Saturn's magnetosphere, *Geophys. Res. Lett., 32*, L14S10, doi:10.1029/2005GL022620.

Jackman, C. M., N. Achilleos, E. J. Bunce, B. Cecconi, J. T. Clarke, S. W. H. Cowley, W. S. Kurth, and P. Zarka, Interplanetary conditions and magnetospheric dynamics during the Cassini orbit insertion fly-through of Saturn's magnetosphere, *J. Geophys. Res.*, *110*, A10212, doi:10.1029/2005JA011054, 2005.

Jackman, C. M., C. T. Russell, D. J. Southwood, C. S. Arridge, N. Achilleos, and M. K. Dougherty (2007), Strong rapid dipolarizations in Saturn's magnetotail: In-situ evidence of reconnection, *Geophys. Res. Lett., 34*, L11203, doi:10.1029/2007GL029764.

Johnson, R. E., H. T. Smith, O. J. Tucker, M. Liu, M. H. Burger, E. C. Sittler, and R. L. Tokar (2006), The Enceladus and OH Tori at Saturn, *Astrophys. J.*, *644*, doi:10.1086/505750.

Jurac, S., R. E. Johnson, J. D. Richardson, C. Paranicas (2001a), Satellite sputtering in Saturn's magnetosphere, *Planet. Space Sci.*, *49*, 319-326.

Jurac, S., R. E. Johnson ,and J. D. Richardson (2001b), Saturn's E-ring and production of the neutral torus, *Icarus*, *149*, 386-396.

Jurac, S., M. A. McGrath, R. E. Johnson, J. D. Richardson, V. M. Vasyliunas, and A. Eviatar (2002), Saturn: Search for a missing water source, *Geophys. Res. Lett., 29*, doi:10.1029/2002GL015855.

Kempf, S., R. Srama, M. Horányi, M. Burton, S. Helfert, G. Moragas-Klostermeyer, M. Roy, and E. Grün (2005), High-velocity streams of dust originating from Saturn, *Nature*, *433*.

Khurana, K. K., M. K. Dougherty, C. T. Russell and J. S. Leisner (2007), Mass loading of Saturn's magnetosphere near Enceladus, *J. Geophys. Res.,* in press, doi:10.1029/2006JA012110.

Kivelson, M. G., K. K. Khurana, C. T. Russell, and R. J. Walker (1997), Intermittent short-duration magnetic field anomalies in the Io torus: Evidence for plasma interchange ?, *Geophys. Res. Lett., 24*, 2127.

Kivelson, M. G. (2006), Does Enceladus govern magnetospheric dynamics at Saturn, *Sci.*, *311*, 1391-1392.

Krimigis, S. M., D. G. Mitchell, D. C. Hamilton, S. Livi, I. Dandouras, S. Jaskulek, T. P. Armstrong, J. D. Boldt, A. F. Cheng, G. Gloeckler, J. R. Hayes, K. C. Hsieh, W.-H. Ip, E. P. Keath, E. Kirsch, N. Krupp, L. J. Lanzerotti, R. Lundgren, B. H. Mauk, R. W. McEntire, E. C. Roelof, C. E. Sclemm, B. E. Tossman, B. Wilken, and D. J. Williams (2004), Magnetospheric Imaging Instrument (MIMI) on the Cassini mission to Saturn/Titan, *Space Sci. Rev.*, *114*, 233.

Krimigis, S. M., D. G. Mitchell, D. C. Hamilton, N. Krupp, S. Livi, E. C. Roelof, I. Dandouras, T. P. Armstrong, B. H. Mauk, C. Paranicas, P. C. Brandt, S. Bolton, A. F. Cheng, T. Choo, G. Cloeckler, J. Hayes, K. C. Hsieh, W.-H. Ip, S. Jaskulek, E. P. Keath, E. Kirsch, M. Kusterer, A. Lagg, L. J. Lanzerotti, D. LaVallee, J. Manweiler, R. W. McEntire, W. Rasmuss, J. Saur, F. S. Turner, D. J. Williams, and J. Woch (2005), Dynamics of Saturn's magnetosphere from the Magnetospheric Imaging Instrument during Cassini's orbital insertion, *Science*, *307*, 1270.

Krimigis, S. M., N. Sergis, D. G. Mitchell, D. C. Hamilton, and N. Krupp (2007), A dynamic, rotating ring current around Saturn, *Nature*, *450*, doi:10.1038/nature06425.

Krupp, N. et al. (2004), Dynamics of the Jovian magnetosphere, in *Jupiter: The Planet, Satellites and Magnetosphere*, Cambridge Planetary Science.

Krupp, N., A. Lagg, J. Woch, S. M. Krimigis, S. Livi, D. G. Mitchell, E. C. Roelof, C. Paranicas, B. H. Mauk, D. C. Hamilton, T. P. Armstrong, and M. K. Dougherty (2005), The Saturnian plasma sheet as revealed by energetic particle measurements, *Geophys. Res. Lett.,* L20S03, doi:10.1029/2005GL022829.

Kurth, W. S., D. A. Gurnett, J. T. Clarke, P. Zarka, M. D. Desch, M. L. Kaiser, B. Cecconi, A. Lecacheux, W. M. Farrell, P. Galopeau, J.-C. Gérard, D. Grodent, R. Prangé, M. K. Dougherty, and F. J. Crary (2005a), An Earth-like correspondence between Saturn's auroral features and radio emission, *Nature*, *433*, 2004.

Kurth, W. S., G. B. Hospodarsky, D. A. Gurnett, B. Cecconi, P. Louarn, A. Lecacheux, P. Zarka, H. O. Rucker, M. Boudjada, and M. L. Kaiser (2005b), High spectral and temporal resolution observations of Saturn Kilometric Radiation, *Geophys. Res. Lett.*, *32*, L20S07, doi:10.1029/2005GL022648.

Kurth, W. S., A. Lecacheux, T. F. averkamp, J. B. Groene, and D. A. Gurnett (2006), A Saturnian longitude system based on a variable kilometric radiation period, *Geophys. Res. Lett., 34*, L02201, doi:10.1029/2006GL028336.

Leisner, J. S., C. T. Russell, K. K. Khurana, M. K. Dougherty, and N. André (2005), Warm flux tubes in the E-ring plasma torus: Initial Cassini magnetometer observations, *Geophys. Res. Lett., 32*, L14S08, doi:10.1029/2005GL022652.

Leisner, J. S., C. T. Russell, M. K. Dougherty, X. Blanco-Cano, R. J. Strangeway, and C. Bertucci (2006), Ion cyclotron waves in Saturn's E ring: Initial Cassini observations, *Geophys. Res. Lett., 33*, L11101, doi:10.1029/2005GL024875.

Leisner, J. S., C. T. Russell, K. K. Khurana, and M. K. Dougherty (2007), Measuring the stress state of the Saturnian magnetosphere, *Geophys. Res. Lett., 34*, L12103,doi:10.1029/2007GL029315.

Louarn, P., D. Gurnett, W. Kurth, G. Hospodarsky, A. Roux, S. Krimigis, D. Mitchell, I. Dandouras, J. Sauvaud, N. Krupp, M. DOugherty, N. André and M. Blanc (2004), Observations of Flux Modulations in SKR and Low-Frequency Waves, Relations with

Other Measurements and Possible Implications on the Magnetospheric Activity, *AGU*, Fall Meeting, abstract P51A-1408.

Luhmann, J., R. E. Johnson, R. L. Tokar, S. A. Ledvina, and T. E. Cravens (2006), A model of the ionosphere of Saturn's rings and its implications, *Icarus*, *181*, 465-474.

Mauk, B. H., D. J. Williams, R. W. McEntire, K. K. Khurana, and J. G. Roederer (1999), Storm-like dynamics of Jupiter's inner and middle magnetosphere, *J. Geophys. Res.*, *104*, doi:10.1029/1999JA900097.

Mauk, B. H., J. Saur, D. G. Mitchell, E. C. Roelof, P. C. Brandt, T. P. Armstrong, D. C. Hamilton, S. M. Krimigis, N. Krupp, S. A. Livi, J. W. Manweiler, and C. P. Paranicas (2005), Energetic particle injections in Saturn's magnetosphere, *Geophys. Res. Lett.*, *32*, L14S05, doi:10.1029/2005GL022485.

Melrose, D. B. (1967), Rotational effects on the distribution of thermal plasma in the magnetosphere of Jupiter, *Planet. Space Sci.*, *15*, 381.

Mitchell, D. G., P. C. Brandt, E. C. Roelof, J. Dandouras, S. M. Krimigis, B. H. Mauk, C. P. Paranicas, N. Krupp, D. C. Hamilton, W. S. Kurth, P. Zarka, M. K. Doughert, E. J. Bunce, and D. E. Shemansky (2005), Energetic ion acceleration in Saturn's magnetotail: Substorms at Saturn ?, *Geophys. Res. Lett.*, *32*, L20S01, doi:10.1029/2005GL022647.

Moncuquet, M., A. Lecacheux, N. Meyer-Vernet, B. Cecconi, and W. S. Kurth (2005), Quasi thermal noise spectroscopy in the inner magnetosphere of Saturn with Cassini/RPWS: Electron temperature and density, *Geophys. Res. Lett.*, *32*, L20S02, doi:10.1029/2005GL022508.

Nimmo, F., J. R. Spencer, R. T. Pappalardo, and M. E. Mullen (2007), Shear heating as the origin of the plumes and heat flux on Enceladus, *Nature*, *447*, doi:10.1038/nature05783.

Paranicas, C., R. B. Decker, B. H. Mauk, S. M. Krimigis, T. A. Armstrong, and S. Jurac (2004), Energetic ion composition in Saturn's magnetosphere revisited, *Geophys. Res. Lett., 31*, L04810, doi:10.1029/2003GL018899.

Parkinson, C. D., M.-C. Liang, H. Hartman, C. J. Hansen, G. Tinetti, V. Meadows, J. L. Kirschvink, and Y. L. Yung (2007), Enceladus: Cassini observations and implications for the search for life, *Astron. Astroph.*, *463*, doi:10.1051/0004-6361:20065773.

Persoon, A. M., D. A. Gurnett, W. S. Kurth, G. B. Hospodarsky, J. B. Groene, P. Canu, and M. K. Dougherty (2005), Equatorial electron density measurements in Saturn's inner magnetosphere, *Geophys. Res. Lett., 32*, L23105.

Porco, C. C., P. Helfenstein, P. C. Thomas, A. P. Ingersoll, J. Wisdom, R. West, G. Neukum, T. Denk, R. Wagner, T. Roatsch, S. Kieffer, E. Turtle, A. McEwen, T. V. Johnson, J. Rathbun, J. Veverka, D. Wilson, J. Perry, J. Spitale, A. Brahic, J. A. Burns, A. D. DelGenio, L. Dones, C. D. Murray, S. Squyres (2006), Cassini Observes the Active South Pole of Enceladus, *Science*, *311*, 5766, doi:10.1126/science.1123013.

Richardson, J. D. (1998), Thermal plasma and neutral gas in Saturn's magnetosphere, *Rev. Geophys., 36*, 501.

Richardson, J. D. and S. Jurac (2005), A self-consistent model of plasma and neutrals at Saturn: The ion tori, *Geophys. Res. Lett., 31*, L24803, doi:10.1029/2004GL020959.

Russell, C. T., K. K. Khurana, D. E. Huddleston, and M. G. Kivelson (1998), Localized reconnection in the near jovian magnetotail, *Sci.*, *280*, 1061.

Russell, C. T., M. G. Kivelson, W. S. Kurth, and D. A. Gurnett (2000), Implications of Depleted Flux Tubes in the Jovian Magnetosphere, *Geophys. Res. Lett., 27*, 3133.

Russell, C. T. (2001), The dynamics of planetary magnetospheres, *Planet. Space Sci.*, *49*, 1005-1030.

Russell, C. T. (2004), Outer planets magnetospheres: a tutorial, *Adv. Space Res.*, *33*, 2004.

Russell, C. T. (Ed.) (2004), *The Cassini-Huygens Mission*, Springer, New York.

Russell, C. T., J. S. Leisner, K. K. Khurana, M. K. Dougherty, X. BLanco-Cano, and J. L. Fox (2005), Ion cyclotron waves in the Saturnian magnetosphere associated with Cassini's engine exhaust, *Geophys. Res. Lett., 32*, L14S01, doi:10.1029/2005GL022672.

Rymer, A. M., B. H. Mauk, T. W. Hill, C. Paranicas, N. André, E. C. Sittler, D. G. Mitchell, H. T. Smith, R. E. Johnson, A. J. Coates, D. T. Young, S. J. Bolton, M. F. Thomsen, and M. K. Dougherty (2007), Electron sources in Saturn's magnetosphere, *J. Geophys. Res., 112*, doi:10.1029/2006JA012017.

Sanchez-Lavega, A. (2005), How long is the day on Saturn ?, *Science*, *307*, 1223.

Shemansky, D. E., P. Matheson, D. T. Hall, H.-Y. Hu, and T. M. Tripp (1993), Detection of the hydroxyl radical in the Saturn magnetosphere, *Nature*, *363*, 329-331.

Sittler, E. C., Jr., K. W. Ogilvie, and J. D. Scudder (1983), Survey of Low-Energy plasma electrons in Saturn's magnetosphere: Voyagers 1 and 2, *J. Geophys. Res., 88*, 8847.

Sittler, E. C., Jr., M. Thomsen, D. Chornay, M. D. Shappirio, D. Simpson, R. E. Johnson, H. T. Smith, A. J. Coates, A. M. Rymer, F. Crary, D. J. McComas, D. T. Young, D. Reisenfeld, M. K. Dougherty, and N. André (2005), Preliminary results on Saturn's inner plasmasphere as observed by Cassini: comparison with Voyager, *Geophys. Res. Lett., 32*, L14S07, doi:10.1029/2005GL022653.

Sittler, E. C., Jr., M. Thomsen, D. Chornay, M. D. Shappirio, D. Simpson, R. E. Johnson, H. T. Smith, A. J. Coates, A. M. Rymer, F. Crary, D. J. McComas, D. T. Young, D. Reisenfeld, M. K. Dougherty, and N. André (2006a), Cassini observations of Saturn's inner plasmasphere: Saturn orbit insertion results, *Planet. Space Sci.*, *54*, doi:10.1016/j.pss.2006.05.038.

Sittler, E. C., Jr., M. Blanc, J. D. Richardson (2006b), Proposed model for Saturn's auroral response to the solar wind: Centrifugal instability model, *J. Geophys. Res.*, *111*, A06208, doi:10.1029/2005JA011191.

Sittler, E. C., R. E. Johnson, H. T. Smith, J. D. Richardson, S. Jurac, M. Moore, J. F. Cooper, B. H. Mauk, M. Michael, C. Paranicas, T. P. Armstrong, and B. Tsurutani (2006c), Energetic nitrogen ions within the inner magnetosphere of Saturn, *J. Geophys. Res., 111*, A09223, doi:10.1029/2004JA010509.

Smith, E. J., L. Davis, D. E. Jones, P. J. Coleman, D. S. Colburn, P. Dyal, C. P. Sonett (1980), Saturn's magnetosphere and its interaction with the solar wind, *J. Geophys. Res., 85*, 5655-5674.

Smith, H. T., M. Shappirio, E. C. Sittler, D. Reisenfeld, R. E. Johnson, R. A. Baragiola, F. J. Crary, D. J. McComas, and D. T. Young (2005), Discovery of nitrogen in Saturn's inner magnetosphere, *Geophys. Res. Lett., 32*, L14S03, doi:10.1029/2005GL022654.

Smith, H. T. (2006), The search for nitrogen in Saturn's magnetosphere, Ph.D. Thesis University of Virginia, Charlottesville, VA.

Southwood, D. J., and M. G. Kivelson (2007), Saturnian mageetospheric dynamics: Elucidation of a camshaft model, *J. Geophys. Res., 112*, A12222, doi:10.1029/2007JA012254.

Spencer, J. R., J. C. Pearl, M. Segura, F. M. Flasar, A. Mamoutkine, P. Romani, B. J. Buratti, A. R. Hendrix, L. J. Spilker and R. M. C. Lopes (2006), Cassini Encounters Enceladus: Background and the Discovery of a South Polar Hot Spot, *Science*, *311*, 5766, doi:10.1126/science.1121661.

Spahn, F., J. Schmidt, N. Albers, M. Hörning, M. Makuch, M. Seiss, S. Kempf, R. Srama, V. Dikarev, S. Helfert, G. Moragas-Klostermeyer, A. V. Krivov, M. Sremcevi, A. J. Tuzzolino, T. Economou, and E. Grün (2006), Cassini dust measurements at Enceladus and implications for the origin of the E ring, *Sci.*, *311*, 1416.

Srama, R., T. J. Ahrens, N. Altobelli, S. Auer, J. G. Bradley, M. Burton, V. V. Dikarev, T. Economou, H. Fechtig, M. Görlich, M. Grande, A. Graps, E. Grün, O. Havnes, S. Helfert, M. Horanyi, E. Ingenbergs, E. K. Jessberger, T. V. Johnson, S. Kempf, A. V. Krivov, H. Krüger, A. Mocker-Ahlreep, g. Moragas-Klostermeyer, P. Lamy, M. Landgraf, D. Linkert, G. Linkert, F. Lura, J. A. M. McDonnell, D. Möhlmann, G. E. Morfill, M. Müller, M. ROy, G. Scäfer, G. Schlotzhauer, G. H. Scwehm, F. Spahn, M. Stübig, J. Svestka, V. Tscherjawski, A. J. Tuzzolino, R. Wäsch, and H. A. Zook (2004), The Cassini Cosmic Dust Analyser, *Space Sci. Rev.*, *114*.

Thorne, R. M., T. P. Armstrong, S. Stone, D. J. Williams, R. P. McEntire, Bolton, D. J., D. A. Gurnett, and M. G. Kivelson (1997), Galileo evidence for rapid interchange transport in the Io torus, *Geophys. Res. Lett., 24*, 2131.

Tokar, R. L., R. E. Johnson, M. F. Thomse, D. M. Delapp, R. A. Baragiola, M. F. Francis, D. B. Reisenfeld, B. A. Fish, D. T. Young, F. J. Crary, A. J. Coates, D. A. Gurnett, and W. S. Kurth (2005), Cassini observations of the thermal plasma in the vicinity of Saturn's main rings and the F and G rings, *Geophys. Res. Lett., 32*, L14S04, doi:10.1029/2005GL022690.

Tokar R. L., R. E. Johnson, T. W. Hill, D. H. Pontius, W. S. Kurth, F. J. Crary, D. T. Young, M. F. Thomsen, D. B. Reisenfeld, A. J. Coates, G. R. Lewis, E. C. Sittler, and D. A. Gurnett (2006), The interaction of the atmosphere of Enceladus with Saturn's plasma, *Sci.*, *311*, 5766.

Wahlund, J.-E., R. Boström, G. Gustafsson, D. A. Gurnett, W. S. Kurth, T. Averkampf, G. B. Hospodarsky, A. M. Persoon, P. Canu, A. Pedersen, M. D. Desch, A. I. Eriksson, R. Gill, M. W. Morooka, and M. André (2005), The inner magnetosphere of Saturn: Cassini RPWS cold plasma results from the first encounter, *Geophys. Res. Lett., 32*, L20S09, doi:10.1029/2005GL022699.

Waite, J. H., W. S. Lewis, W. T. Kasprzak, V. G. Anicich, B. P. Block, T. E. Cravens, G. G. Fletcher, W.-H. Ip, J. G. Luhmann, R. L. McNutt, H. B. Niemann, J. K. Parejko, J. E. Richards, R. L. Thorpe, E. M. Walter, R. V. Yelle, The Cassini Ion and Neutral Mass Spectrometer (INMS) Investigation, *Space Sci. Rev.*, *114*, 113.

Waite, J. H., T. E. Cravens, W.-H. Ip, W. T. Kasprzak, J. G. Luhmann, R. L. McNutt, H. B. Niemann, R. V. Yelle, I. Mueller-Wodarg, S. A. Ledvina, and S. Scherer (2005), Cassini Ion and Neutral Measurements of Oxygen Ions near Saturn's A ring, *Science*, *307*, 1260.

Waite, J. H., M. R. Combi, W.-H. Ip, T. E. Cravens, R. L. McNutt, W. Kasprzak, R. Yelle, J. Luhmann, H. Niemann, D. Gell, B. Magee, G. Fletcher, J. Lunine, and W.-L. Tseng (2006), Cassini Ion and Neutral Mass Spectrometer Enceladus plume composition and structure, *Sci.*, *311*, 1419.

Wang, Z., D. A. Gurnett, T. F. Averkamp, A. M. Persoon, and W. S. Kurth (2006), Characteristics of dust particles detected near Saturn's ring plane with the Cassini Radio and Plasma Wave instrument, *Planet. Space Sci.*, *54*, 10.1016/j.pss.2006.05.015.

Warwick, J. W., J. B. Pearce, D. R. Evans, T. D. Carr, J. J. Schauble, J. K. Alexander, M. L. Kaiser, M. D. Desch, M. Pedersen, A. Lecacheux, G. Daigne, A. Boishot, and C. H. Barrow (1981], Planetary radio astrononmy observations from Voyager 1 at Saturn, *Sci.*, *212*, 239-243.

Xin, L., D. A. Gurnett, O. Santolik, W. S. Kurth, and G. B. Hospodarsky (2006), Whistler-mode auroral hiss emissions observed near Saturn's B ring, *J. Geophys. Res., 111*, A06214, doi:10.1029/2005JA011432.

Young, D. T.,J.-J. Berthelier, M. Blanc, J. L. Burch, A. J. Coates, R. Goldstein, M. Grande, T. W. Hill, R. E. Johnson, V. Kelha, D. J. McComas, E. C. Sittler, K. R. Svenes, K. Szegö, P. Tanskanen, K. Ahola, D. Anderson, S. Bakshi, R. A. Baragiola, B. L. Barraclough, R. K. Black, S. Bolton, T. Booker, R. Bowman, P. Casey, F. J. Crary, D. Delapp, G. Dirks, N. Eaker, H. Funsten, J. D. Furman, J. T. Gosling, H. Hannula, C. Holmlund, H. Huomo, J. M. Illiano, P. Jensen, M. A. Johnson, D. R. Linder, T. Luntama, S. Maurice, K. P. McCave, K. Mursula, B. T. Narheim, J. E. Nordholt, A. Preece, J. Rudzki, A. Ruitberg, K. Smith, S. Szalai, M. F. Thomsen, K. Viherkanto, J. Vilppola, T. Vollmer, T. E. Wahl, M. Wüest, T. Ylikorpi, C. Zinsmeyer (2004), Cassini Plasma Spectrometer investigation, *Space Sci. Rev.*, *114*.

Young, D. T., J. J. Berthelier, M. Blanc, J. L. Burch, S. Bolton, A. J. Coates, F. J. Crary, R. Goldstein, M. Grande, T. W. Hill, R. E. Johnson, R. A. Baragiola, V. Kelha, D. J. McComas, K. Mursula, E. C. Sittler, K. R. Svenes, K. Szegö, P. Tanskanene,

M. F. Thomsen, S. Baksji, B. L. Barraclough, Z. Bebesi, D. Delapp, M. W. Dunlop, J. T. Gosling, J. D. Furman, L. K. Gilbert, D. Glenn, C. Holmlund, J.-M. Illiano, G. R. Lewis, D. R. Linder, S. Maurice, H. J. McAndrews, B. T. Narheim, E. Pallier, D. Reisenfeld, A. M. Rymer, H. T. Smith, R. L. Tokar, J. Vilppola and C. Zinsmeyer (2005), Composition and dynamics of plasma in Saturn's magnetosphere, *Science*, *307*, 1262.

Zarka, P. (1998), Auroral radio emissions at the outer planets: Observations and theories, *J. Geophys. Res., 103*, 20,159.

Zarka, P., L. Lamy, R. Prangée, and H. O. Rucker (2007), Modulation of Saturn's radio clock by solar wind speed, *Nature*, *450*, 7167, doi:10.1038/nature06237.

Figure 1. Left: Spacecraft trajectories in the (X, Y) Kronocentric Solar Magnetospheric (KSM) plane. The KSM coordinate system has Saturn at the origin, with the X axis directed towards the Sun, Z (pointing northward) defined such that Saturn's rotation and magnetic axis lies in the XZ plane, and Y lying in Saturn's rotational and equatorial plane. An average magnetopause boundary model (thick solid line) is taken from *Arridge et al.* [2006]. Right: Spacecraft trajectories in the $((X^2+Y^2)^{\frac{1}{2}}, Z)$ Kronographic (KG) plane. The KG coordinate system is analogous to the geographic (longitude and latitude) system used at the Earth. The X axis points along the Saturn Prime Meridian as defined by the IAU, Y lies in the rotational equatorial plane and Z lies along the rotation axis. Distance units are in Saturn radii (R_s= 60,268 km).

Figure 2. Multi-instrumental view of the Saturnian magnetosphere, from June 30 00:00 UT (DOY 182) to July 2 (DOY 184) 00:00 UT. From top to bottom: Color-coded MIMI LEMMS energy (in logarithmic scale)-time spectrograms of 1) electron and 2) ion intensities (in logarithmic scale, $cm^{-2}sr^{-1}s^{-1}keV^{-1}$); 3) MAG magnetic field components in a Saturn-centered polar spherical coordinate system (the radial one in blue, $-B_r$; the theta one in red, B_θ; and the azimuthal one in green B_ϕ) and magnitude (in black, B_m); Color-coded 4) CAPS ELS and 5) IMS energy (in logarithmic scale)-time spectrograms of electron and ion counts (in logarithmic scale); and 6) Color-coded (in logarithmic scale) RPWS electric field frequency (in logarithmic scale)-time spectrogram, versus time (in hours) and radial distance (in R_s). Vertical lines are used in section 5 to describe a unified picture of the four different magnetospheric regions and delineate their boundaries. CA indicates Closest Approach. The locations of some of Saturn's moons are indicated in the first panel and repeated in the second one. Notations for moons: Ti, Titan; Rh: Rhea; Di: Dione; En: Enceladus; Mi: Mimas.

Figure 3. Comparison of *Sittler et al.*'s [1983] illustration of Saturn's magnetosphere at noon (as defined from low-energy ($<$ 6 keV) electron plasma observations) with the new Cassini CAPS inbound (June, 30) observations. Cold (1-100 eV) regions are colored blue and hot (100-1000 eV) regions are purple in the schematic. Superimposed on the Cassini inbound trajectory are the CAPS ELS and IMS energy-time spectrograms used in Figure 2.

Figure 4. Same as on Figure 2, but with dedicated emphasize on observations described in the text. 1) Ring ionosphere; 2) Electron plasma above the rings; 3) Energetic particles absorption by ring particles; 4) Radiation belts; 5) Dust impacts; 6) Water magnetosphere; 7) Ion cyclotron waves from engine exhaust (cf., *Russell et al.*, [2005]); 8) Depletion of hot electrons and charge exchange processes; 9) Unusual magnetic flux tubes; 10) Density cavities; 11) Energy-time dispersed injection of hot plasma; 12) Modulations of whistler-mode waves.

Figure 5. Plasma over the rings, observed on July 1 between 03:28 and 04:15 UT. From top to bottom: 1) Left: Color-coded RPWS electric field frequency (in linear scale)-time spectrogram, Right: CAPS IMS ion densities and RPWS total electron densities; 2) MIMI LEMMS pitch angle (in degrees)-time spectrogram of 28-49 keV electron intensities (normalized to maximum), 3) CAPS IMS energy (in logarithmic scale)-time spectrogram of ion counts (in logarithmic scale), 4) ring picture, courtesy of the ISS team; 5) CAPS ELS energy (in logarithmic scale)-time spectrogram of electron counts (in logarithmic scale), along Cassini trajectory. The magenta dashed vertical line delineates the location of the Saturnian synchronous orbit, the black dotted lines the Cassini division boundaries and the black dashed line the Encke gap. The green and solid vertical lines delineate the time intervals corresponding to the observations represented in panel 1.

Figure 6. Observations of an empty flux tube on June 30 between 20:00 and 22:00 UT. From top to bottom: 1) RPWS electric field frequency (in logarithmic scale)-time spectrogram, 2) CAPS ELS and 3) IMS energy (in logarithmic scale)-time spectrograms; 4)-6) MAG VHM magnetic field perturbations (compressional δB_m and transverse ($\delta B_\perp$) field-aligned components, based on Saturn-centered polar spherical coordinates). In this particular field-aligned coordinate system, the perturbed compressional component (along the background magnetic field) is denoted by $\delta B_\|$, and the two transverse components by $\delta B_{\perp_1}$ (approximately opposite to the corotational azimuthal direction) and $\delta B_{\perp_2}$ (approximately opposite to the radial direction and consequently along the radius of curvature of the magnetic field lines), respectively.

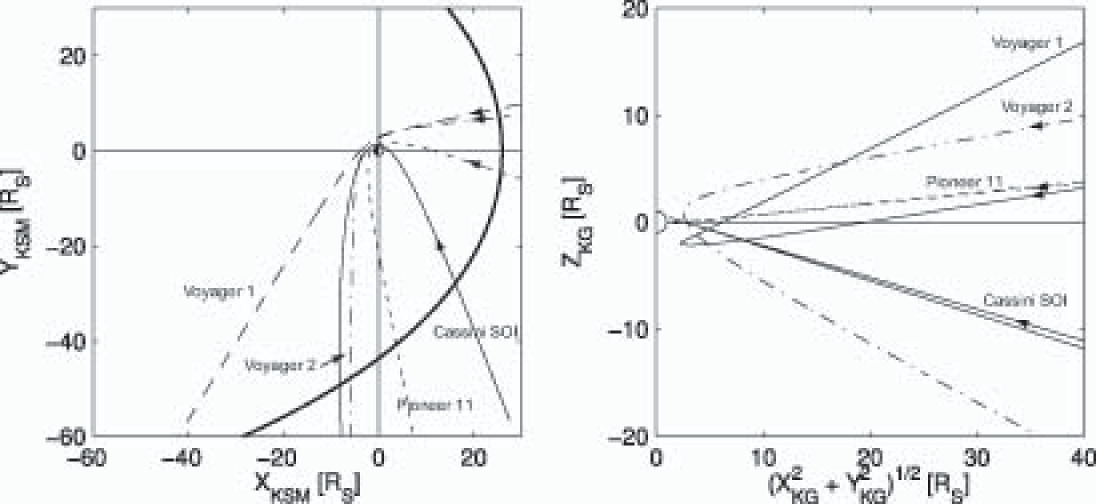

Voyager 1
Voyager 2
Pioneer 11
Cassini SOI
Y_{KSM} [R_S]
X_{KSM} [R_S]
Voyager 1
Voyager 2
Pioneer 11
Cassini SOI
Z_{KG} [R_S]
$(X_{KG}^2 + Y_{KG}^2)^{1/2}$ [R_S]

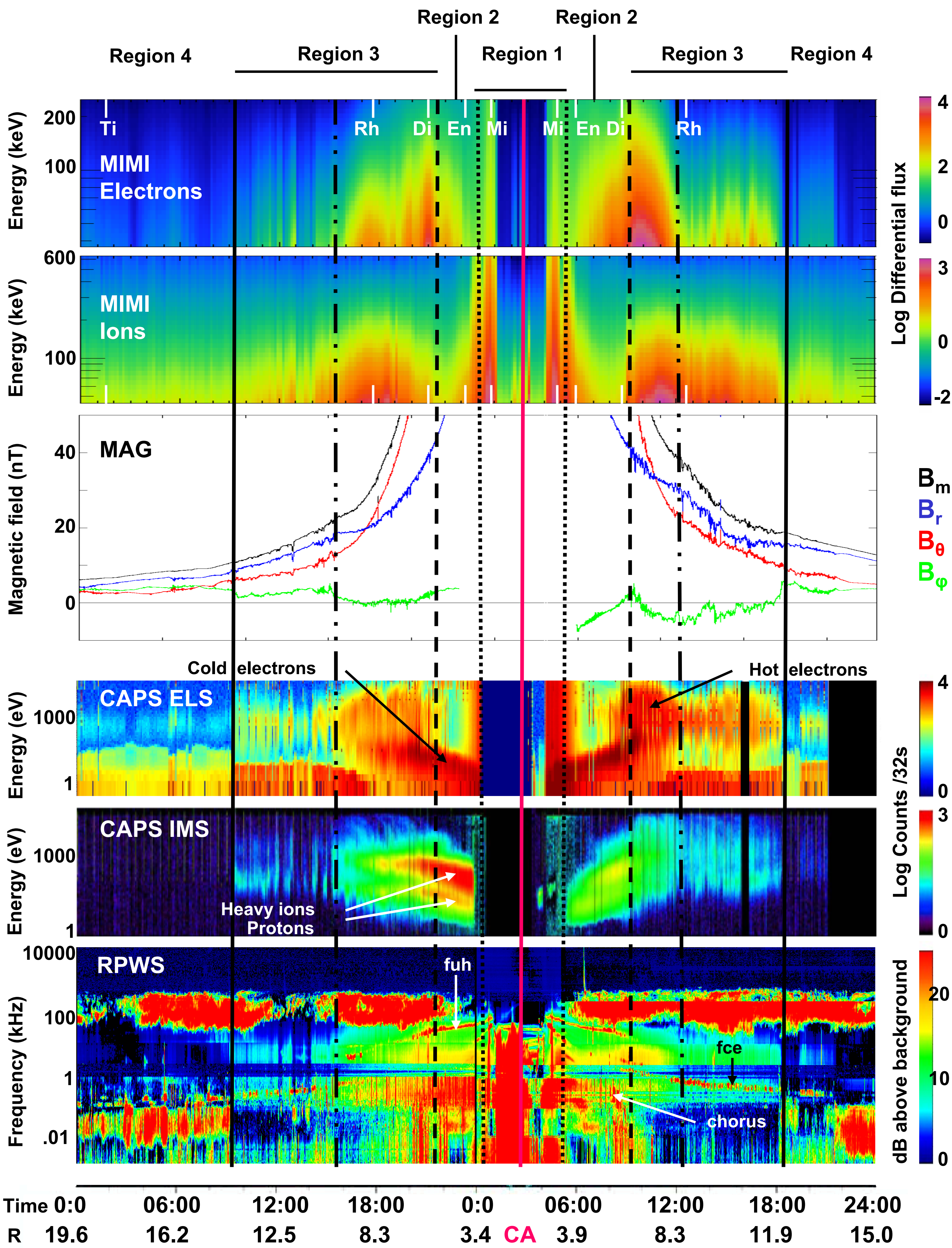

Region 4
Region 3
Region 2
Region 1
Region 2
Region 3
Region 4
Ti
Rh
Di
En
Mi
Mi
En
Di
Rh
MIMI Electrons
MIMI Ions
Energy (keV)
Log Differential flux
MAG
Magnetic field (nT)
B_m
B_r
B_θ
B_φ
Cold electrons
Hot electrons
CAPS ELS
CAPS IMS
Energy (eV)
Heavy ions
Protons
Log Counts /32s
RPWS
fuh
fce
chorus
Frequency (kHz)
dB above background
Time 0:0 06:00 12:00 18:00 0:0 06:00 12:00 18:00 24:00
R 19.6 16.2 12.5 8.3 3.4 CA 3.9 8.3 11.9 15.0

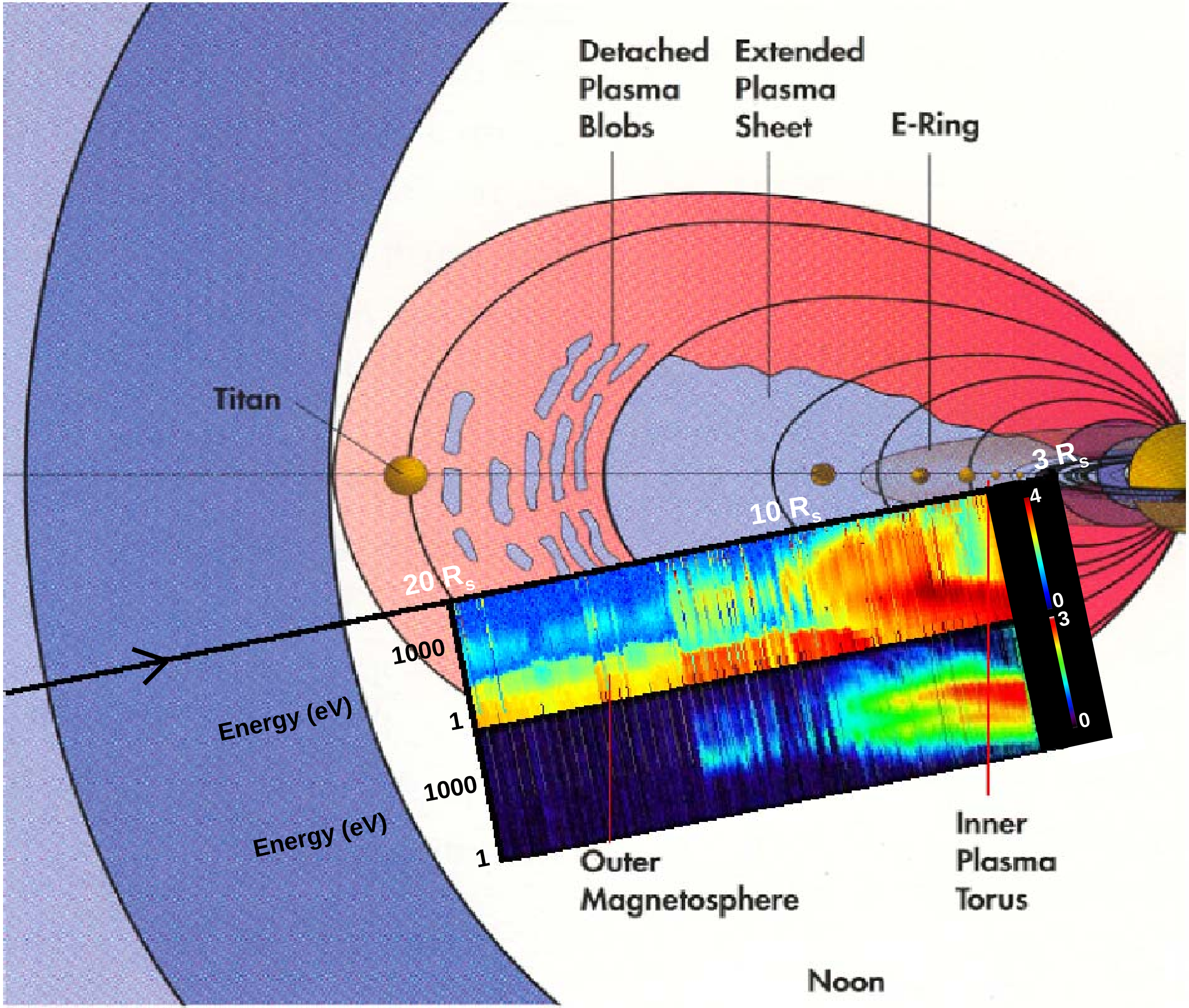

Detached
Plasma
Blobs
Extended
Plasma
Sheet
E-Ring
Titan
3 R$_S$
10 R$_S$
20 R$_S$
4
0
3
0
1000
1
Energy (eV)
1000
1
Energy (eV)
Outer
Magnetosphere
Inner
Plasma
Torus
Noon

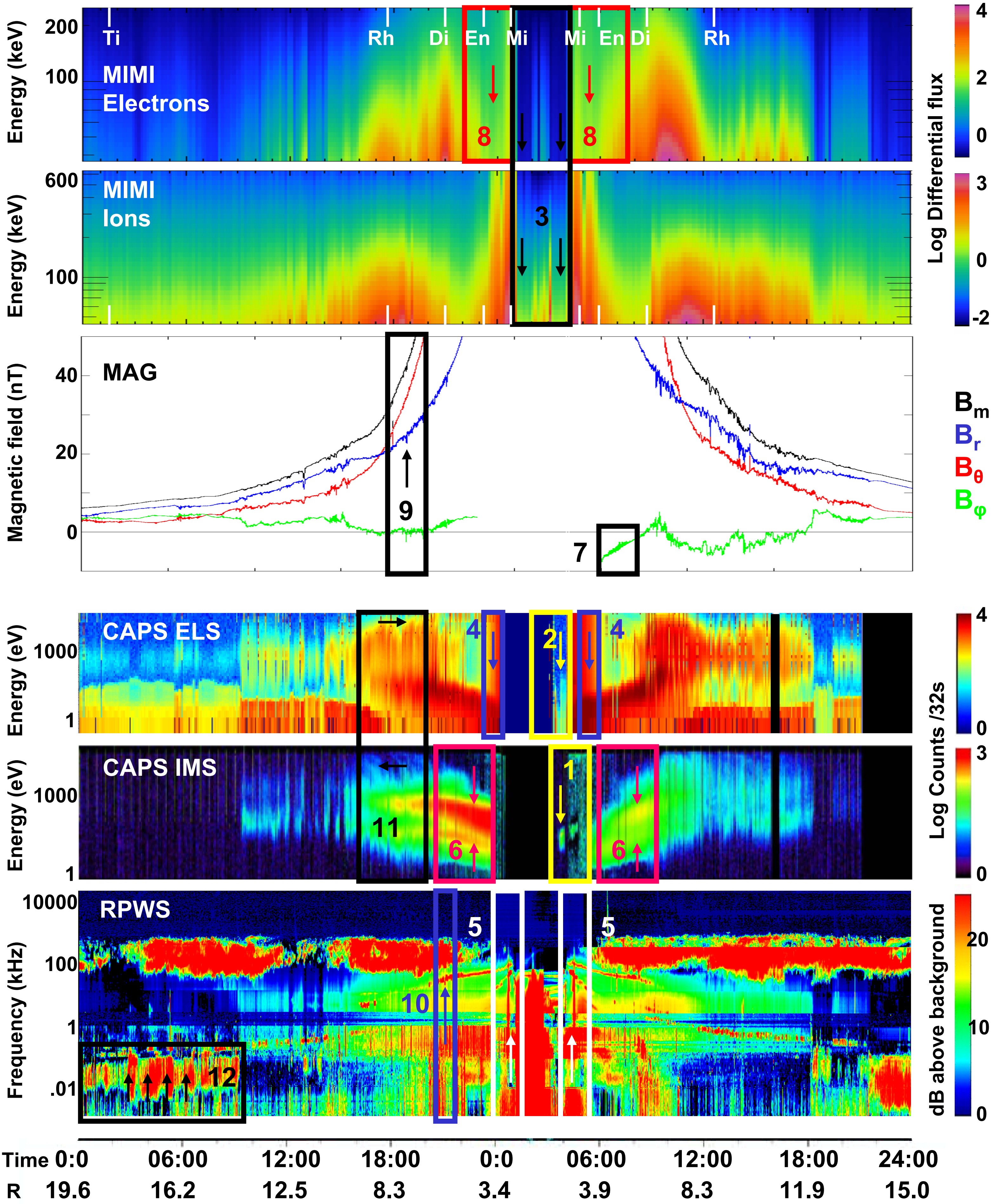

Ti Rh Di En Mi Mi En Di Rh
MIMI Electrons
MIMI Ions
Energy (keV)
Log Differential flux
MAG
Magnetic field (nT)
B_m B_r B_θ B_φ
CAPS ELS
CAPS IMS
Energy (eV)
Log Counts /32s
RPWS
Frequency (kHz)
dB above background
Time 0:0 06:00 12:00 18:00 0:0 06:00 12:00 18:00 24:00
R 19.6 16.2 12.5 8.3 3.4 3.9 8.3 11.9 15.0

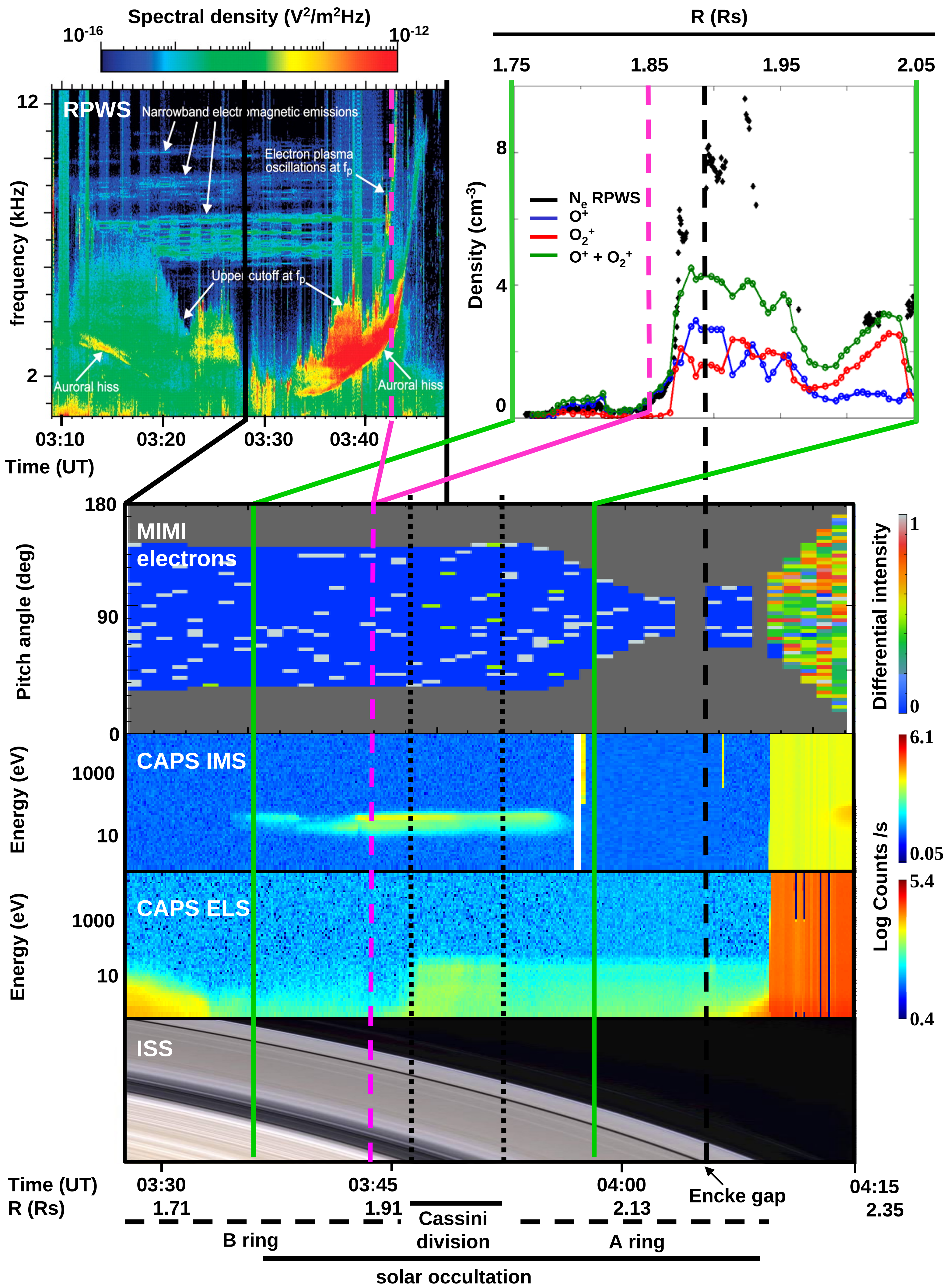

Spectral density (V²/m²Hz)
10⁻¹⁶
10⁻¹²
RPWS
Narrowband electromagnetic emissions
Electron plasma oscillations at fp
Upper cutoff at fp
Auroral hiss
Auroral hiss
frequency (kHz)
12
2
03:10
03:20
03:30
03:40
Time (UT)
R (Rs)
1.75
1.85
1.95
2.05
Density (cm⁻³)
8
4
0
Ne RPWS
O⁺
O₂⁺
O⁺ + O₂⁺
MIMI electrons
Pitch angle (deg)
180
90
0
Differential intensity
1
0
CAPS IMS
Energy (eV)
1000
10
6.1
0.05
CAPS ELS
Energy (eV)
1000
10
5.4
0.4
Log Counts /s
ISS
Time (UT)
R (Rs)
03:30
1.71
03:45
1.91
04:00
2.13
04:15
2.35
Encke gap
B ring
Cassini division
A ring
solar occultation

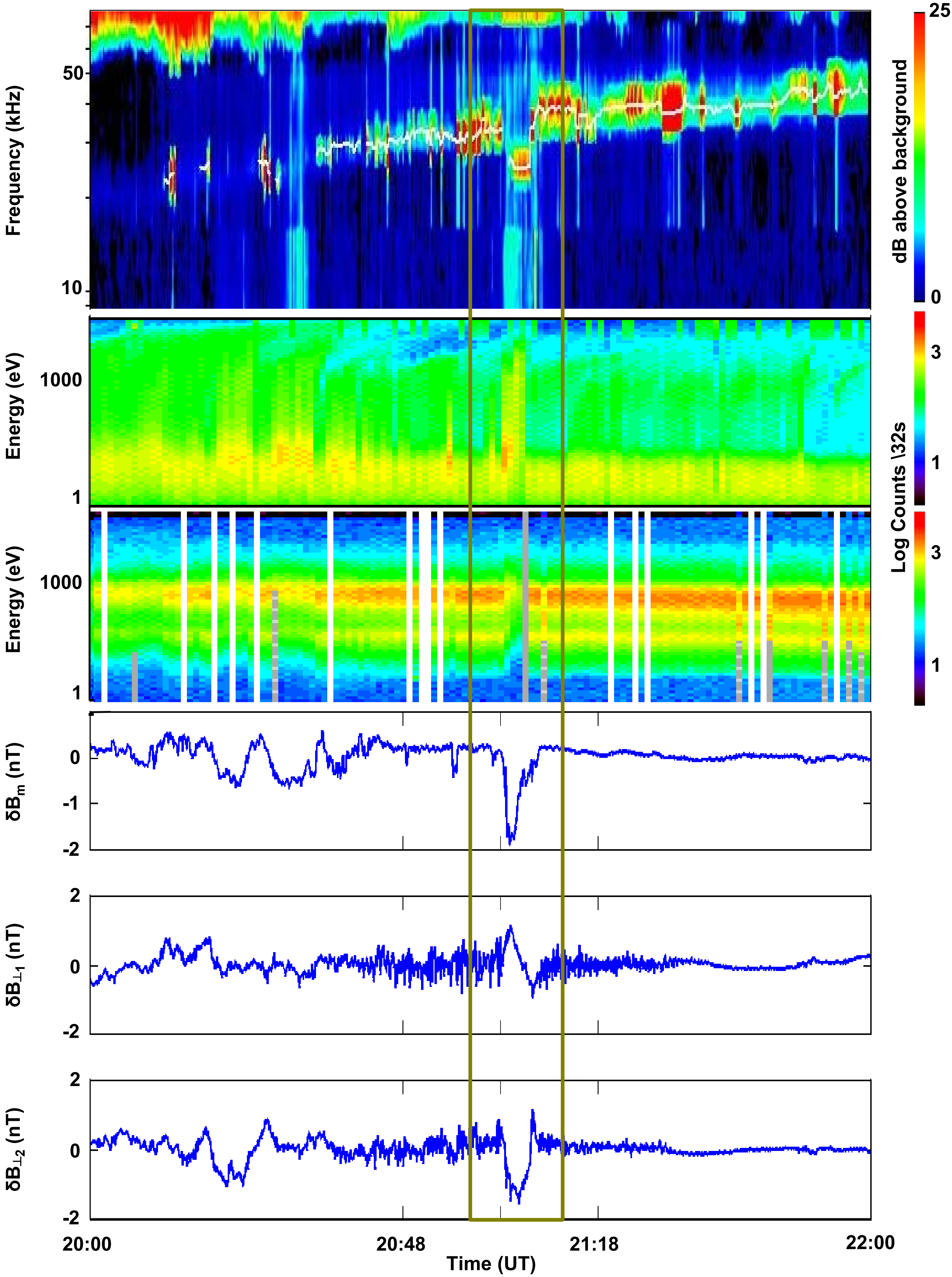

Frequency (kHz)
50
10
dB above background
25
0
Energy (eV)
1000
1
Log Counts \32s
3
1
Energy (eV)
1000
1
3
1
δB_m (nT)
0
-1
-2
δB_⊥1 (nT)
2
0
-2
δB_⊥2 (nT)
2
0
-2
20:00
20:48
21:18
22:00
Time (UT)